Synthesis and Structures of Mono- and Bis(amidinate) Complexes of Aluminum

Martyn P. Coles, Dale C. Swenson, and Richard F. Jordan*

Department of Chemistry, The University of Iowa, Iowa City, Iowa 52242

Victor G. Young, Jr.

Department of Chemistry, The University of Minnesota, Minneapolis, Minnesota 55455

Received July 24, 1997[⊗]

The synthesis and structures of mono- and bis(amidinate) aluminum complexes are described. The reaction of $AlMe_3$ and 1 equiv of carbodiimide, R′N═C═NR′, affords $\{MeC(NR'_2)_2\}AlMe_2$ (**1a**, R′ = ^{i}Pr; **1b**, R′ = Cy = cyclohexyl). The reaction of R′N═C═NR′ with MeLi or ^{t}BuLi generates $Li[RC(NR'_2)_2]$ (**2a**, R = Me, R′ = ^{i}Pr; **3a**, R = ^{t}Bu, R′ = ^{i}Pr; **3b**, R = ^{t}Bu, R′ = Cy; **3c**, R = ^{t}Bu, R′ = $SiMe_3$). **2a**, **3a**, and **3b** may be isolated or reacted *in situ*, while attempted isolation of **3c** gave $[Li(^tBuCN)\{\mu\text{-}N(SiMe_3)_2\}]_2$ (**3d**). The reaction of 1 equiv of $AlCl_3$ with **2a** or **3a**−**c** affords $\{RC(NR'_2)_2\}AlCl_2$ (**4a**, R = Me; **5a**−**c**, R = ^{t}Bu), and the reaction of $AlMe_2Cl$ with **3a**−**c** affords $\{^tBuC(NR'_2)_2\}AlMe_2$ (**6a**−**c**). Alkylation of **5a**,**b** with 2 equiv of $PhCH_2MgCl$ or Me_3CCH_2Li yields $\{^tBuC(NR'_2)_2\}Al(CH_2Ph)_2$ (**7a**,**b**) or $\{^tBuC(NR'_2)_2\}Al(CH_2CMe_3)_2$ (**8a**,**b**). The reaction of 0.5 equiv of $AlCl_3$ with **2a** or **3a**,**b** yields $\{RC(NR'_2)_2\}_2AlCl$ (**9a**, R = Me; **10a**,**b**, R = ^{t}Bu). Complexes **1b**, **3d**, **4a**, **5a**,**b**, **6b**, **8b**, **9a**, and **10a**,**b** have been characterized by X-ray crystallography. The crystallographic results establish that steric interactions between the R and R′ groups influence the R′−N−Al angle and, hence, the steric environment at aluminum.

Introduction

Group 13 compounds incorporating amidinate ligands ($RC(NR'_2)^-$) have been studied intensively in recent years.[1−9] The most important classes of group 13 amidinate compounds are mono(amidinate) $\{RC(NR'_2)\}MX_2$ species (X = halide, alkyl, etc.), which adopt distorted tetrahedral structures, and bis(amidinate) $\{RC(NR'_2)_2\}_2MX$ species, which adopt distorted trigonal-bipyramidal (tbp) structures. Representative examples include the mono(amidinate) compounds $\{MeC(N^iPr)_2\}MMe_2$ (M = Al, Ga, In, Tl),[1] $\{MeC(NSiMe_3)_2\}MMe_2$ (M = Al, Ga, In, Tl),[1,2] $\{PhC(NSiMe_3)_2\}AlCl_2$,[3] and $\{RC(NR'_2)\}GaMe_2$ (R = Ph, Me; R′ = Ph, 4-Cl-C_6H_4, 4-Me-C_6H_4)[4] and the bis(amidinate) compounds $\{PhC(NSiMe_3)_2\}_2AlX$ (X = Cl, H),[5] $\{MeC(NCy)_2\}_2InX$ (X = Cl, Me),[6] and $\{PhC(NPh)_2\}_2GaMe$.[4] Several tris(amidinate) complexes $\{RC(NR'_2)_2\}_3M$ are known, including $\{RC(NPh)_2\}_3Ga$ (R = Me, Ph)[4] and $\{MeC(NCy)_2\}_3In$.[6] In all of these systems, the amidinate ligands are coordinated in a reasonably symmetrical bidentate fashion. There are also several examples of dinuclear group 13 complexes with bridging amidinate ligands, including $[\{\mu\text{-}RC(NH)_2\}_2GaMe_2]_2$ (R = Ph, ^{t}Bu),[4] $[\{\mu\text{-}MeC(NMe)_2\}_2MMe_2]_2$ (M = Al, Ga),[7] and $[\{\mu\text{-}HC(NCy)_2\}_2InMe]_2$.[8] In these cases, the amidinate ligand contains at least one sterically undemanding substituent, suggesting that steric factors influence the preference for chelating versus bridging structures.

Group 13 amidinate compounds are of interest as precursors to nitride materials and as selective reagents and catalysts.[4,5] Additionally, amidinate ligands are useful for fundamental studies of the relationships between ligand structure and metal coordination geometry, because their steric and (to a lesser extent) electronic properties can be modified by variation of the C- and N-substituents.[6,8,9] Amidinate ligands have been used extensively in other main group, transition metal, and *f*-block coordination chemistry,[10] and parallels to carboxylate RCO_2^- and triazenate $N(NR)_2^-$ ligands have been noted.[11,12]

Our efforts in this area are focused on the chemistry of three-coordinate, six-electron, cationic group 13 complexes of the general type $(L-X)MX^+$ (L−X$^-$ = an

[⊗] Abstract published in *Advance ACS Abstracts,* November 1, 1997.

(1) Kottmair-Maieron, D.; Lechler, R.; Weidlein, J. *Z. Anorg. Allg. Chem.* **1991**, *593*, 111.
(2) Lechler, R.; Hausen, H.-D.; Weidlein, J. *J. Organomet. Chem.* **1989**, *359*, 1.
(3) Ergezinger, C.; Weller, F.; Dehnicke, K. *Z. Naturforsch.* **1988**, *43b*, 1621.
(4) Barker, J.; Blacker, N. C.; Phillips, P. R.; Alcock, N. W.; Errington, W.; Wallbridge, M. G. H. *J. Chem. Soc., Dalton Trans.* **1996**, 431.
(5) Duchateau, R.; Meetsma, A.; Teuben, J. H. *J. Chem. Soc., Chem. Commun.* **1996**, 223.
(6) Zhou, Y.; Richeson, D. S. *Inorg. Chem.* **1996**, *35*, 2448.
(7) Hausen, H.-D.; Gerstner, F.; Schwarz, W. *J. Organomet. Chem.* **1978**, *145*, 277.
(8) Zhou, Y.; Richeson, D. S. *Inorg. Chem.* **1996**, *35*, 1423.
(9) Zhou, Y.; Richeson, D. S. *Inorg. Chem.* **1997**, *36*, 501.
(10) (a) Edelmann, F. T. *Coord. Chem. Rev.* **1994**, *137*, 403. (b) Barker, J.; Kilner, M. *Coord. Chem. Rev.* **1994**, *133*, 219. (c) *The Chemistry of Amidinates and Imidinates*; Patai, S., Ed.; Wiley: New York, 1991; Vol. 2.
(11) Taylor, M. J.; Tuck, D. G. In *Comprehensive Coordination Chemistry*; Wilkinson, G., Gillard, R. D., McCleverty, J. A., Eds.; Pergamon: Oxford, 1987; Vol. 3, pp 105−182. Oldham, C. *Prog. Inorg. Chem.* **1968**, *10*, 223. Casellato, U.; Vigato, P. A.; Vidali, M. *Coord. Chem. Rev.* **1978**, *26*, 85. Mehrotra, R. C.; Bohra, R. *Metal Carboxylates*; Academic: London, 1983. Oldham, C. *Comprehensive Coordination Chemistry*; Wilkinson, G., Ed.; Pergamon: Oxford, 1987; Vol. 2, pp 435−459. For group 13 carboxylate examples, see: Weidlein, J. *J. Organomet. Chem.* **1969**, *16*, P33. Coates, G. E.; Hayter, R. G. *J. Chem. Soc.* **1953**, 2519. Coates, G. E.; Mukherjee, R. N. *J. Chem. Soc.* **1964**, 1295. Hausen, H.-D. *J. Organomet. Chem.* **1972**, *39*, C37.

S0276-7333(97)00632-8 CCC: $14.00

Scheme 1

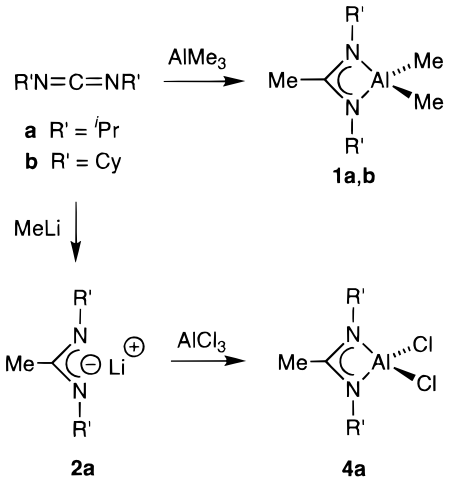

Scheme 2

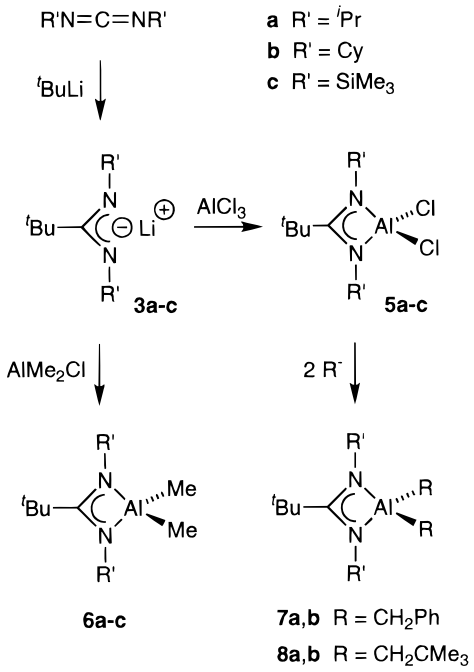

anionic, bidentate, four-electron donor), which are of interest for applications in synthesis and catalysis. It was envisioned that amidinates would serve as appropriate "spectator" ligands for compounds of this type, because they have the required charge and metal binding properties and can be sterically and electronically modified. In this paper, we describe the synthesis and structures of an extensive set of $\{RC(NR')_2\}AlX_2$ (X = Cl, alkyl) and $\{RC(NR')_2\}_2AlCl$ compounds which contain bulky amidinate ligands. The influence of the C−*R* and N−*R*′ substituents on the steric environment at Al is discussed. The conversion of $\{RC(NR')_2\}AlX_2$ compounds to $\{RC(NR')_2\}AlX^+$ cations is described elsewhere.[13]

Results and Discussion

Synthesis of Aluminum Amidinate Complexes. Aluminum amidinate complexes have been synthesized by addition of aluminum alkyls to carbodiimides and by reaction of aluminum halides with preformed amidinate reagents.[1,2,5] We have exploited these general routes to prepare an extensive series of mono- and bis(amidinate) aluminum alkyl and halide compounds.

$\{MeC(NR')_2\}AlX_2$ Complexes. Addition of R′N=C=NR′ (R′ = ^{i}Pr, Cy) to $AlMe_3$ in hexane results in an exothermic reaction and formation of $\{MeC(NR')_2\}AlMe_2$ (**1a**, R′ = ^{i}Pr; **1b**, R′ = Cy, Scheme 1).[14] Compound **1a** is isolated as a pale yellow liquid by removal of the volatiles. **1b** is a low-melting solid that can be purified by sublimation. Alternatively, the reaction of ^{i}PrN=C=N^{i}Pr with MeLi (Et_2O, 0 °C) yields $Li[MeC(N^iPr)_2]$ (**2a**), which can be isolated as a white solid in good yield. Addition of 1 equiv of $AlCl_3$ to **2a** (Et_2O, −78 °C) yields $\{MeC(N^iPr)_2\}AlCl_2$ (**4a**).

$\{^tBuC(NR')_2\}AlX_2$ Complexes. The ^{t}Bu−amidinate reagents $Li[^tBuC(NR')_2]$ (**3a**, R′ = ^{i}Pr; **3b**, R′ = Cy; **3c**, R′ = $SiMe_3$) are formed by the reaction of ^{t}BuLi with the appropriate carbodiimide (Et_2O, 0 °C, Scheme 2). **3a** and **3b** can be isolated in good yield as pale yellow amorphous solids. In contrast, attempts to isolate **3c** yielded the rearrangment product $[Li(^tBuCN)\{\mu\text{-}N(SiMe_3)_2\}]_2$ (**3d**, *vide infra*), and therefore, **3c** was generated *in situ* for use in subsequent reactions. The reaction of **3a**−**c** with 1 equiv of $AlCl_3$ or $AlMe_2Cl$ (Et_2O, −78 °C) yields $\{^tBuC(NR')_2\}AlCl_2$ (**5a**−**c**) or $\{^tBuC(NR')_2\}AlMe_2$ (**6a**−**c**, Scheme 2). Compounds **5a**−**c** are isolated as crystalline solids by recrystallization from pentane or toluene. Compounds **6a** and **6c** are isolated as colorless crystals by sublimation (50−55 °C), and **6b** is isolated as colorless crystals by recrystallization from pentane.

The reaction of **5a**,**b** with 2 equiv of $PhCH_2MgCl$ or $LiCH_2CMe_3$ (Et_2O, −78 °C; Scheme 2) affords $\{^tBuC(NR')_2\}Al(CH_2Ph)_2$ (**7a**,**b**) and $\{^tBuC(NR')_2\}Al(CH_2CMe_3)_2$ (**8a**,**b**). Compounds **7a**,**b** are initially isolated as colorless liquids by extraction with pentane and removal of the volatiles but solidify upon storage at −40 °C. In contrast, **8a**,**b** are isolated directly as white solids.

NMR Spectroscopic Properties of $\{RC(NR')_2\}AlX_2$ Complexes. The ^{1}H and ^{13}C NMR spectra of the $\{RC(NR')_2\}AlX_2$ (X = Cl, alkyl) complexes described above are consistent with C_{2v}-symmetric structures and symmetrical bidentate coordination of the amidinate ligand. The ^{13}C NMR Al−*C* signals of the dialkyl complexes are broad due to the ^{27}Al quadrupole and exhibit low $^1J_{CH}$ values (104−114 Hz).

X-ray Crystallographic Analysis of $\{RC(NR')_2\}AlX_2$ Complexes. Crystal data for selected $\{RC(NR')_2\}AlX_2$ complexes are summarized in Table 1, refinement details are discussed in the Experimental Section, and selected bond distances are collected in Tables 2 and 3. The molecular geometries and atom-labeling schemes are shown in Figures 1−6, and selected bond angles are given in Figure 7.

(12) Vrieze, K.; Van Koten, G. In *Comprehensive Coordination Chemistry*; Wilkinson, G., Ed.; Pergamon: Oxford, 1987; Vol. 2, pp 189−244. For group 13 triazenate examples, see: Leman, J. T.; Barron, A. R.; Ziller, J. W.; Kren, R. M. *Polyhedron* **1989**, *8*, 1909. Leman, J. T.; Barron, A. R. *Organometallics* **1989**, *8*, 1828. Leman, J. T.; Roman, H. A.; Barron, A. R. *J. Chem. Soc., Dalton Trans.* **1992**, 2183. Leman, J. T.; Roman, H. A.; Barron, A. R. *Organometallics* **1993**, *12*, 2986. Leman, J. T.; Braddock-Wilking, J.; Coolong, A. J.; Barron, A. R. *Inorg. Chem.* **1993**, *32*, 4324.

(13) Coles, M. P.; Jordan, R. F. *J. Am. Chem. Soc.* **1997**, *119*, 8125.

(14) Complex **1a** was prepared previously by the reaction of ^{i}PrN=C=N^{i}Pr, MeLi and $AlMe_2Cl$; see ref 1.

Table 1. Summary of Crystal Data for Compounds 4a, 5a,b, 1b, 6b, and 8b

complex	**4a**	**5a**	**5b**	**1b**	**6b**	**8b**
formula	$C_8H_{17}AlCl_2N_2$	$C_{11}H_{23}AlCl_2N_2$	$C_{17}H_{31}AlCl_2N_2$	$C_{16}H_{31}AlN_2$	$C_{19}H_{37}AlN_2$	$C_{27}H_{53}AlN_2$
fw	239.12	281.19	361.32	278.41	320.49	432.69
cryst size, mm	0.50 × 0.35 × 0.18	0.45 × 0.37 × 0.37	0.35 × 0.29 × 0.13	0.67 × 0.54 × 0.35	0.43 × 0.38 × 0.27	0.54 × 0.52 × 0.38
color/shape	colorless/plate	colorless/prism	colorless/fragment	colorless/fragment	colorless/fragment	colorless/fragment
d (calcd), Mg/m^3	1.216	1.175	1.194	1.031	1.055	1.004
cryst syst	triclinic	orthorhombic	monoclinic	triclinic	monoclinic	monoclinic
space group	$P\bar{1}$	Pnma	*C*2/*c*	$P\bar{1}$	*C*2/*c*	*C*2/*c*
a, Å	7.7223(1)	14.724(4)	13.372(4)	10.253(3)	26.882(9)	28.675(5)
b, Å	8.1224(3)	11.273(3)	11.421(2)	10.841(3)	10.117(2)	11.608(2)
c, Å	10.7338(3)	9.575(2)	13.595(5)	8.775(2)	17.715(5)	18.310(4)
α, deg	95.189(2)			97.77(2)		
β, deg	91.609(1)		104.53(2)	109.55(2)	123.15(2)	110.02(2)
γ, deg	102.806(1)			96.72(2)		
V, Å^3	653.02(3)	1589.3(7)	2009.8(10)	896.8(4)	4034(2)	5726(2)
Z	2	4	4	2	8	8
T, K	173(2)	213(2)	203(2)	210(2)	213(2)	213(2)
diffractometer	Siemens SMART Platform CCD	Enraf-Nonius CAD4	Enraf-Nonius CAD4	Enraf-Nonius CAD4	Enraf-Nonius CAD4	Enraf-Nonius CAD4
radiation, *λ*, Å	Mo Kα, 0.710 73	Mo Kα, 0.710 73	Mo Kα, 0.710 73	Mo Kα, 0.710 73	Mo Kα, 0.710 73	Mo Kα, 0.710 73
2*θ* range, deg	3.8 < 2*θ* < 50.0	5.0 < 2*θ* < 50.0	4.0 < 2*θ* < 55.0	4.0 < 2*θ* < 50.0	4.0 < 2*θ* < 55.0	4.2 < 2*θ* < 55.0
data colld: *h*;*k*;*l*	±9; ±9; 0,12	−17,1; −11,13; −11,1	−17,16; ±14; −1,17	±12; ±12; ±10	±34; −13,4; −22,19	-37,35; −15,9; −1,23
no. of reflns	3607	3044	4382	5410	6564	8751
no. of unique reflns	2271	1464	2240	3131	4438	6431
R_{int}	0.0168	0.0225	0.0292	0.0316	0.0602	0.0272
no. of obsd reflns	*I* > 2*σ*(*I*), 1946	*I* > 2*σ*(*I*), 1033	*I* > 2*σ*(*I*), 1114	*I* > 2*σ*(*I*), 2581	*I* > 2*σ*(*I*), 3566	*I* > 2*σ*(*I*), 4682
μ, mm^{-1}	0.529	0.444	0.366	0.105	0.101	0.085
transmission range, %	82−100	95−100	85−100	80−100	78−100	99−100
structure solution	direct methods[a]	direct methods[b]	direct methods[b]	direct methods[b]	direct methods[b]	direct methods[b]
GOF on F^2	1.090	1.070	0.978	1.109	1.063	1.076
R indices (*I* > 2*σ*(*I*))	R1 = 0.0425,[c] wR2 = 0.1160[d]	R1= 0.0523,[c] wR2 = 0.1237[d]	R1= 0.0449,[c] wR2 = 0.1187[d]	R1 = 0.0517,[c] wR2 = 0.1427[d]	R1 = 0.0562,[c] wR2 = 0.1442[d]	R1 = 0.0487,[c] wR2 = 0.1232[d]
R indices (all data)	R1 = 0.0505,[c] wR2 = 0.1207[d]	R1= 0.0759,[c] wR2 = 0.1409[d]	R1= 0.1149,[c] wR2 = 0.1609[d]	R1 = 0.0638,[c] wR2 = 0.1576[d]	R1 = 0.0699,[c] wR2 = 0.1635[d]	R1 = 0.0775,[c] wR2 = 0.1469[d]
max resid density, e/Å^3	0.26	0.49	0.31	0.30	0.52	0.31

[a] *SHELXTL-Plus, Version 5*; Siemens Industrial Automation, Inc.: Madison, WI. [b] *MULTAN, Multan80*; University of York: York, England. [c] $R1 = \sum||F_o| - |F_c||/\sum|F_o|$. [d] $wR2 = [\sum[w(F_o^2 - F_c^2)^2]/\sum[w(F_o^2)^2]]^{1/2}$, where $w = [\sigma^2(F_o^2) + (aP)^2 + bP]^{-1}$.

Table 2. Selected Bond Lengths (Å) for 4a and 5a,b

	{MeC(N^{i}Pr)$_2$}AlCl$_2$ (**4a**)		
Al(1)−N(1)	1.879(2)	Al(1)−N(2)	1.879(2)
Al(1)−Cl(1)	2.1078(11)	Al(1)−Cl(2)	2.1057(10)
N(1)−C(4)	1.339(3)	N(1)−C(7)	1.457(3)
N(2)−C(4)	1.336(3)	N(2)−C(2)	1.464(3)
C(4)−C(5)	1.495(3)		
	{^{t}BuC(N^{i}Pr)$_2$}AlCl$_2$ (**5a**)[a]		
Al(1)−N(1)	1.872(3)	Al(1)−N(2)	1.863(3)
Al(1)−Cl(1)	2.1036(14)	N(1)−C(5)	1.335(5)
N(1)−C(1)	1.476(6)	N(2)−C(5)	1.340(5)
N(2)−C(3)	1.462(5)	C(5)−C(6)	1.540(5)
	{^{t}BuC(NCy)$_2$}AlCl$_2$ (**5b**)[b]		
Al(1)−N(1)	1.870(2)	Al(1)−Cl(1)	2.1018(14)
N(1)−C(21)	1.347(3)	N(1)−C(1)	1.480(8)

[a] Symmetry transformations used to generate equivalent atoms: $x, -y + {}^1/_2, z$. [b] Symmetry transformations used to generate equivalent atoms: $-x, y, -z + {}^1/_2$.

Table 3. Selected Bond Lengths (Å) for 1b, 6b, and 8b

	{MeC(NCy)$_2$}AlMe$_2$ (**1b**)		
Al(1)−N(1)	1.923(2)	Al(1)−N(2)	1.926(2)
Al(1)−C(15)	1.957(3)	Al(1)−C(16)	1.958(3)
N(1)−C(13)	1.329(3)	N(1)−C(1)	1.451(2)
N(2)−C(13)	1.325(2)	N(2)−C(7)	1.445(3)
C(13)−C(14)	1.496(3)		
	{^{t}BuC(NCy)$_2$}AlMe$_2$ (**6b**)		
Al(1)−N(1)	1.927(2)	Al(1)−N(2)	1.9124(14)
Al(1)−C(18)	1.958(2)	Al(1)−C(19)	1.950(2)
N(1)−C(13)	1.343(2)	N(1)−C(1)	1.456(2)
N(2)−C(13)	1.339(2)	N(2)−C(7)	1.454(2)
C(13)−C(14)	1.540(2)		
	{^{t}BuC(NCy)$_2$}Al(CH$_2$CMe$_3$)$_2$ (**8b**)		
Al(1)−N(1)	1.9276(14)	Al(1)−N(2)	1.939(2)
Al(1)−C(18)	1.992(2)	Al(1)−C(23)	2.002(3)
N(1)−C(13)	1.343(2)	N(1)−C(1)	1.464(2)
N(2)−C(13)	1.346(2)	N(2)−C(7)	1.462(2)
C(13)−C(14)	1.545(2)		

The dichloride complexes **4a** and **5a**,**b** adopt distorted tetrahedral structures. The amidinate bite angle (N−Al−N) is rather acute (70.91° average) which is compensated for by opening of the N−Al−Cl angles (117.51° average). The dialkyl complexes **1b**, **6b**, and **8b** also adopt distorted tetrahedral structures with similar N−Al−N bite angles (68.74° average) and N−Al−C angles (115.34° average). The Cl−Al−Cl angles (110.61° average) in **4a** and **5a**,**b** are close to the ideal tetrahedral angle of 109.47°, but the C−Al−C angles in **1b**, **6b**, and **8b** are ca. 8° larger (117.42° average). The average Al−Cl and Al−CH_3 cone angles are estimated to be 56.3° and 51.0°, respectively, for these compounds, and therefore, the Cl−Al−Cl angles in **4a** and **5a**,**b** would be predicted to be slightly larger the the C−Al−C angles on the basis of steric effects.[15] The smaller values for the Cl−Al−Cl angles can be rationalized in terms of simple VSEPR concepts; i.e., the Al−Cl bonding electron pair is smaller than the Al−CH_3 bonding electron pair due to the higher electronegativity of Cl versus C. Alternatively, the bond angle trend can be rationalized in terms of hybridization effects; i.e., the smaller values for the Cl−Al−Cl angles reflect increased p-character

(15) The Al−Cl and Al−CH_3 cone angles were estimated using crystallographic data for **1b**, **4a**, **5a**, **5b**, and **6b**, and Van der Waals radii were taken from Bondi, A. *J. Phys. Chem.* **1964**, *68*, 441.

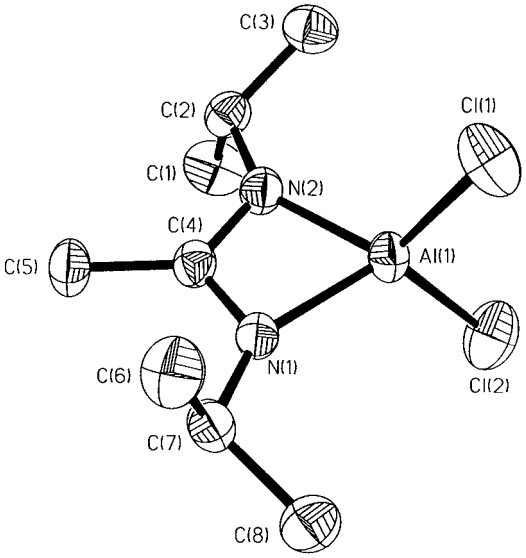

Figure 1. Molecular structure of $\{MeC(N^iPr)_2\}AlCl_2$ (**4a**, H-atoms omitted).

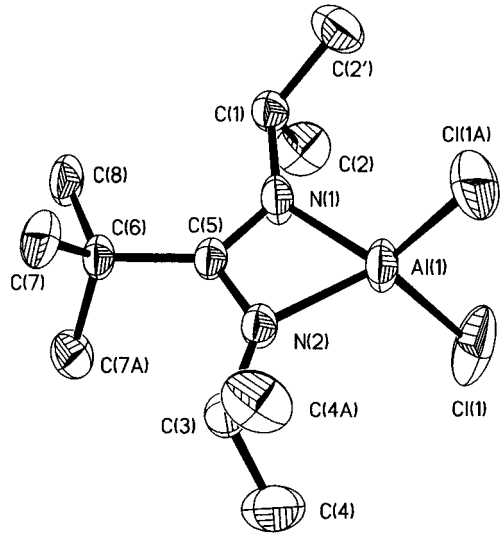

Figure 2. Molecular structure of $\{^tBuC(N^iPr)_2\}AlCl_2$ (**5a**, H-atoms omitted).

in the Al hybrid orbitals used in bonding to the electronegative chlorine ligands (Bent's Rule).[16] The Al−N bond distances are essentially equal within each molecule and are shorter for the dichlorides (1.87 Å average) than for the dialkyl species (1.93 Å average) due to the stronger electron-donor ability of Me vs Cl. These Al−N bond distances are comparable to those in $\{MeC(NSiMe_3)_2\}AlMe_2$ (1.93 Å)[2] and $\{PhC(NSiMe_3)_2\}AlCl_2$ (1.88 Å).[3] The Al−Cl bond distances in **4a** and **5a**,**b** (2.10 Å average) are comparable to the Al−Cl distances in $AlCl_3$ (2.06 Å, gas phase)[17] and Al_2Cl_6 (terminal Al−Cl = 2.07 Å).[18] The Al−Me distances in **1b** and **6b** (1.96 Å average) are comparable to the terminal Al−Me bond distance in Al_2Me_6 (1.97 Å average).[19]

In all of the $\{RC(NR')_2\}AlX_2$ compounds studied, the $\{RC(NR')_2\}Al$ core forms a nearly planar metallacycle (|N−Al−N−C torsion angles| < 2.1°). The amidinate

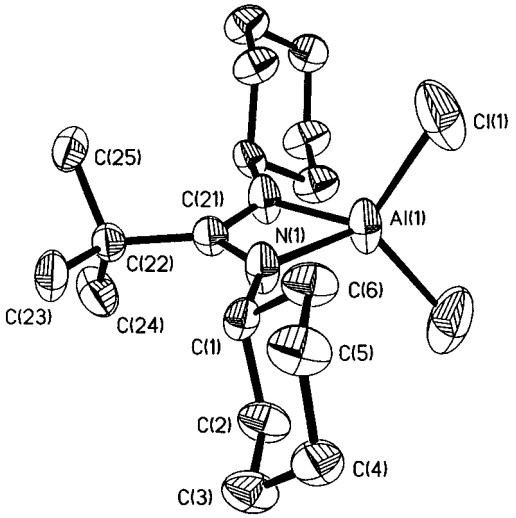

Figure 3. Molecular structure of $\{^tBuC(NCy)_2\}AlCl_2$ (**5b**, H-atoms omitted).

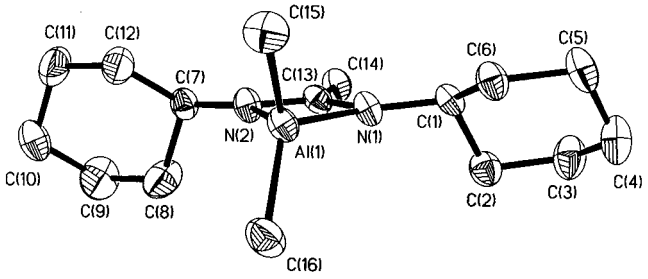

Figure 4. Molecular structure of $\{MeC(NCy)_2\}AlMe_2$ (**1b**, H-atoms omitted).

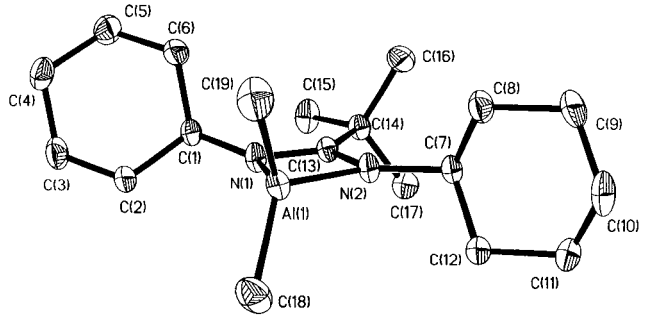

Figure 5. Molecular structure of $\{^tBuC(NCy)_2\}AlMe_2$ (**6b**, H-atoms omitted).

carbon and nitrogen atoms exhibit distorted trigonal-planar coordination (sum of angles ca. 360°). The arrangement of the substituents around these atoms is not symmetrical; in particular, the N−C−N bond angle is reduced to 107.4−110.4°. The two C−N distances (1.34 Å average) are essentially equal within each molecule and are in the range observed for delocalized systems such as pyridine (d(C−N) = 1.34 Å).[20] The C−N distances are intermediate between C=N double bond distances in carbodiimides (1.16−1.22 Å)[21] and C(sp^2)−N single bond distances (1.47 Å).[22] The value of the C−N bond distances, together with the equality of the C−N distances, and of the Al−N distances

(16) Bent, H. A. *J. Chem. Educ.* **1960**, *37*, 616. Bent, H. A. *Chem. Rev.* **1961**, *61*, 275.
(17) Zasorin, E. Z.; Rambidi, N. G. *Zh. Strukt. Khim.* **1967**, *8*, 391.
(18) Greenwood, N. N.; Earnshaw, A. In *Chemistry of the Elements*; Pergamon: Oxford, 1984; pp 264 and 289.
(19) Vranka, R. G.; Amma, E. L. *J. Am. Chem. Soc.* **1967**, *89*, 3121.
(20) Allen, F. H.; Kennard, O.; Watson, D. G.; Brammer, L.; Orpen, G. A.; Taylor, R. *J. Chem. Soc., Perkin Trans. 2* **1987**, S1.
(21) Obermeyer, A.; Kienzle, A.; Weidlein, J.; Riedel, R.; Simon, A. *Z. Anorg. Allg. Chem.* **1994**, *620*, 1357 and references cited therein.
(22) Sutton, L. E. *Interatomic Distances and Configuration in Molecules and Ions*; Special Publications No. 18; The Chemical Society: London, 1965.

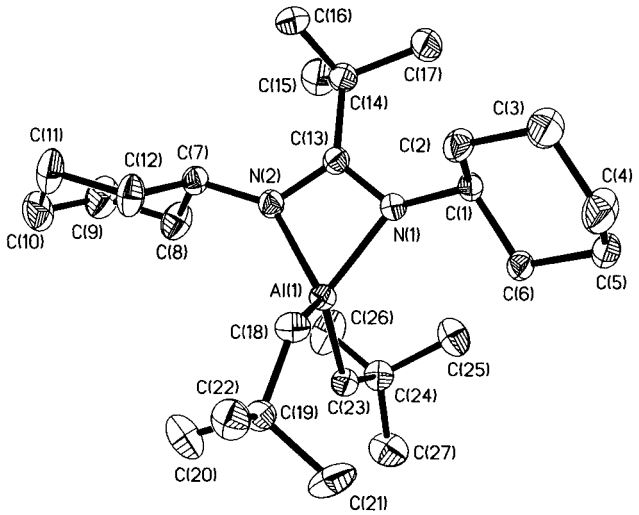

Figure 6. Molecular structure of {^{t}BuC(NCy)$_2$}Al(CH$_2$CMe$_3$)$_2$ (**8b**, H-atoms omitted).

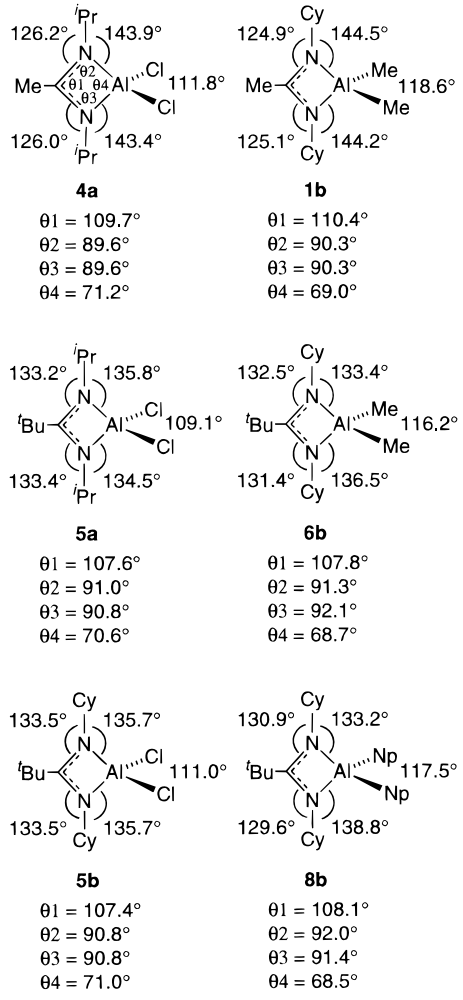

Figure 7. Schematic representation of the core structures of {RC(NR′)$_2$}AlX$_2$ compounds **4a**, **5a**,**b**, **1b**, **6b** and **8b**. The angles Θ1, Θ2, Θ3, and Θ4 are defined in the same manner for each compound and are indicated for **4a**. Np = CH$_2$CMe$_3$.

establish that the bonding in the N−C═N unit is delocalized.

One important aspect of our work on cationic aluminum amidinate complexes is control of steric crowding at the Al center.[13] Comparison of key bond angles within the {RC(NR′)$_2$}Al core as a function of the C−*R* and N−*R*′ substituents provides insight to this issue (Figure 7). The primary effect of replacing a Me group at the central carbon with a ^{t}Bu group is a decrease in the R′−N−Al angle, which results in greater crowding at Al. The ^{i}Pr−N−Al angle in {^{t}BuC(N^{i}Pr)$_2$}AlCl$_2$ (**5a**, 135.2° average) is 8.5° smaller than that in {MeC(N^{i}Pr)$_2$}-AlCl$_2$ (**4a**; 143.7° average). The trigonal-planar arrangement about nitrogen is retained and the alkyl substituents remain in the plane of the metallacycle in both structures. The shortest H−H distances between the C−*R* and the N−*R*′ groups in **4a** is 2.22 Å, which is slightly less than the sum of the van der Waals radii (2.4 Å). In **5a**, the shortest C−R/N−R′ H−H distance is 1.86 Å, indicating that significant steric interactions between the R and R′ groups are present. Neither complex exhibits close contacts between the ^{i}Pr groups and the chloride ligands. Changing the N-*R*′ group from ^{i}Pr (**5a**) to cyclohexyl (**5b**) has a minimal effect on the structure of the metallacycle core. Analogous structural trends are observed in the dialkyl complexes. The Cy−N−Al angle in {^{t}BuC(NCy)$_2$}AlMe$_2$ (**6b**, 134.9°) is 9.4° smaller than that in {MeC(NCy)$_2$}-AlMe$_2$ (**1b**, 144.3°) as a result of close H−H contacts between C−*R* and N−*R*′ (shortest H−H contacts, **1b** = 2.21 Å, **6b** = 1.99 Å).

{RC(NR′)$_2$}$_2$AlCl Complexes. The reaction of AlCl$_3$ with 2 equiv of **2a** or **3a**,**b** (Et$_2$O, −50 °C) results in clean formation of {MeC(N^{i}Pr)$_2$}$_2$AlCl (**9a**) or {^{t}BuC(NR′)$_2$}$_2$AlCl (**10a**,**b**; eq 1). These compounds are isolated as analytically pure white or pale yellow crystalline solids by recrystallization from pentane. X-ray crystallographic analyses (*vide infra*) establish that **9a** and **10a**,**b** adopt distorted tbp structures with approximate C_2 symmetry, as indicated in eq 1. For the isopropyl-substituted cases **9a** and **10a**, the two isopropyl groups on a given amidinate ligand are inequivalent and the two Me groups within each isopropyl group are diasterotopic in a static idealized tbp structure. Rotation of the amidinate ligands will exchange the isopropyl groups, and inversion of configuration at Al will exchange the Me groups within each isopropyl group. The ^{1}H and ^{13}C NMR spectra of **9a** and **10a** each contain a single set of amidinate resonances and a single isopropyl methyl resonance, indicating that inversion of configuration at Al is rapid on the NMR time scale at ambient temperature. Cooling a sample of **10a** to −80 °C does not resolve the inequivalent alkyl groups in the ^{1}H NMR spectrum. The ^{1}H and ^{13}C NMR spectra of **10b** are also consistent with rapid inversion at Al at ambient temperature.

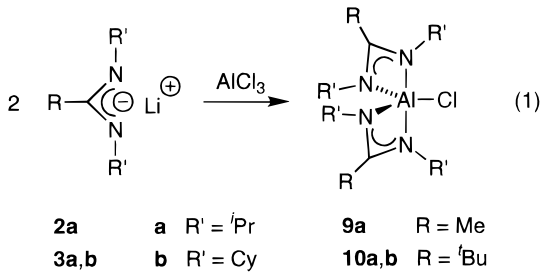

X-ray Crystallographic Analysis of {RC(NR′)$_2$}$_2$AlCl Complexes. Crystal data for **9a** and **10a**,**b** are summarized in Table 4, and selected bond distances and angles are collected in Table 5. Molecular geometries and atom-labeling schemes are shown in Figures 8−10, and details of the structure refinements

Table 4. Summary of Crystal Data for Compounds 9a and 10a,b

complex	**9a**	**10a**	**10b**
formula	$C_{16}H_{34}AlClN_4$	$C_{22}H_{46}AlClN_4$	$C_{70.5}H_{130}Al_2Cl_2N_8$
fw	344.90	429.06	1214.69
cryst size, mm	0.20 × 0.20 × 0.15	0.54 × 0.42 × 0.39	0.56 × 0.43 × 0.41
color/shape	colorless/prism	colorless/prism	colorless/prism
d (calcd), Mg/m^3	1.154	1.078	1.117
cryst syst	monoclinic	monoclinic	monoclinic
space group	$C2/c$	$P2_1/c$	$P2_1/c$
a, Å	11.6149(5)	19.777(3)	33.066(9)
b, Å	12.8226(6)	9.3100(10)	10.676(2)
c, Å	14.0189(6)	15.208(2)	20.958(6)
β, deg	108.054(1)	109.230(10)	102.46(2)
V, Å^3	1985.1(2)	2643.9(6)	7224(3)
Z	4	4	4
T, K	173(2)	203(2)	213(2)
diffractometer	Siemens SMART Platform CCD	Enraf-Nonius CAD4	Enraf-Nonius CAD4
radiation, λ, Å	Mo Kα, 0.710 73	Mo Kα, 0.710 73	Mo Kα, 0.710 73
2θ range, deg	4.8 < 2θ < 50.0	4.0 < 2θ < 55.0	4.0 < 2θ < 50.0
data colld: $h;k;l$	±13; 0,15; 0,16	±25; −12,1; −18,19	−38,39; −1,12; −24,6
no. of reflns	4915	7540	16 306
no. of unique reflns	1753	5885	12 315
R_{int}	0.0280	0.0127	0.0205
no. of obsd reflns	$I > 2\sigma(I)$, 1462	$I > 2\sigma(I)$, 4708	$I > 2\sigma(I)$, 8976
μ, mm^{-1}	0.240	0.192	0.159
transmission range, %	86−100	98−100	98−100
structure solution	direct methods[a]	direct methods[b]	direct methods[b]
GOF on F^2	1.089	1.083	1.044
R Indices ($I > 2\sigma(I)$)	R1 = 0.0441,[c] wR2 = 0.1152[d]	R1 = 0.0374,[c] wR2 = 0.0987[d]	R1 = 0.0439,[c] wR2 = 0.1089[d]
R Indices (all data)	R1 = 0.0563,[c] wR2 = 0.1214[d]	R1 = 0.0538,[c] wR2 = 0.1107[d]	R1 = 0.0778,[c] wR2 = 0.1374[d]
max resid density, e/Å^3	0.27	0.26	0.50

[a] *SHELXTL-Plus, Version 5*, Siemens Industrial Automation, Inc.: Madison, WI. [b] *MULTAN*, *Multan80*; University of York: York, England. [c] $R1 = \sum||F_o| - |F_c||/\sum|F_o|$. [d] $wR2 = [\sum[w(F_o^2 - F_c^2)^2]/\sum[w(F_o^2)^2]]^{1/2}$, where $w = [\sigma^2(F_o^2) + (aP)^2 + bP]^{-1}$.

are discussed in the Experimental Section. Complexes **9a** and **10a**,**b** adopt distorted tbp structures in which both bidentate amidinate ligands occupy an equatorial and an axial site, and the remaining equatorial site is occupied by the chloride ligand. The acute amidinate bite angle (67.39° average) causes a significant reduction of the $N_{ax}-Al-N_{ax}$ angles (range 163.83−166.47°) and a smaller reduction of the $N_{eq}-Al-N_{eq}$ angles (range 110.3−118.0°) from the ideal tbp values of 180° and 120°. As expected for tbp geometry, the $Al-N_{ax}$ bonds are longer than the corresponding $Al-N_{eq}$ bonds (e.g., for **9b**, Al−N(1) = 2.041(2) Å, Al−N(2) = 1.914(2) Å).[23] The lengthening of the $Al-N_{ax}$ bond is accompanied by a slight shortening (ca 0.02 Å) of the $C-N_{ax}$ bond versus the $C-N_{eq}$ bonds within the amidinate ligands,[5,24] while the Al−N−C−N rings remain nearly planar (|N−Al−N−C torsion angles| < 2.4°). The {RC(NR′)$_2$}Al bonding may be represented by resonance structures **A** and **B** in Chart 1. The deviations from symmetrical coordination observed for **9a** and **10a**,**b** correspond to an increased contribution from structure **B**. Replacing the methyl substituent at the central carbon atom with a ^{t}Bu group has the same effect as that observed for the {RC(NR′)$_2$}AlX$_2$ complexes; i.e., the N−alkyl groups are pushed more toward the Al center in the ^{t}Bu derivatives. This effect is more pronounced for the axial than the equatorial position (e.g., **9a**, ax ^{i}Pr−N−Al = 147.6°, eq ^{i}Pr−N−Al = 140.8°; **10a**, ax ^{i}Pr−N−Al = 136.4° average, eq ^{i}Pr−N−Al = 137.9° average).

Structure of [Li(^{t}BuCN){μ-N(SiMe$_3$)$_2$}]$_2$ (3d). As noted above, attempted isolation of **3c** yielded a new compound **3d**. The NMR data for **3d** are inconsistent with an amidinate structure. The ^{1}H NMR spectra of **3d** in C_6D_6, CD_2Cl_2, or THF-d_8 contain singlets for the ^{t}Bu and $SiMe_3$ groups in the expected 1:2 ratio, but the $SiMe_3$ resonance is broadened in the latter solvent. Additionally, the ^{13}C NMR spectrum (THF-d_8) lacks a low-field amidinate N*C*N signal (cf. δ 168 for **3a** and **3b**).

The molecular structure of **3d** was established by X-ray crystallography (Figure 11). Crystal data for **3d** are summarized in Table 6, details of the structure solution and refinement are provided in the Experimental Section, and selected bond distances and angles are collected in Table 7. The structure of **3d** consists of two Li(^{t}BuCN)$^+$ cations linked by bridging N(SiMe$_3$)$_2^-$ groups; i.e., **3d** is formulated as the dimer [Li(^{t}BuCN){μ-N(SiMe$_3$)$_2$}]$_2$. The Li_2N_2 core is symmetrical and planar with distorted trigonal-planar geometry at Li and distorted tetrahedral geometry at N. The nitrile ligands lie in the Li_2N_2 plane. Analogous structures have been observed for other lithium amide complexes, e.g., [Li(OEt$_2$){μ-N(SiMe$_3$)$_2$}]$_2$,[25] [Li(Base){μ-N(CH$_2$Ph)$_2$}]$_2$ (Base = Et$_2$O, hmpa),[26] and [Li{μ-N(SiMe$_3$)$_2$}]$_2$.[27]

It is likely that **3d** forms by rearrangement of **3c** by a net 1,3 $SiMe_3$ shift, as shown in Scheme 3. The driving force for this reaction is unknown at present; however, relief of steric crowding is unlikely to be the sole cause, as **5c** and **6c** which contain ^{t}BuC(NSiMe$_3$)$_2^-$ ligands are stable species, and the crystal structure of {^{t}BuC(NSiMe$_3$)$_2$}$_2$SnCl$_2$ was recently reported.[9] Other lithium amidinates have been isolated without re-

(23) Albright, T. A.; Burdett, J. K.; Whangbo, M. H. *Orbital Interactions in Chemistry*; Wiley: New York, 1985; Chapter 14.
(24) Ergezinger, C.; Weller, F.; Dehnicke, K. *Z. Naturforsch., Teil B* **1988**, *43*, 1119.
(25) (a) Engelhardt, L. M.; May, A. S.; Raston, C. L.; White, A. H. *J. Chem. Soc., Dalton Trans.* **1983**, 1671. (b) Lappert, M. F.; Slade, M. J.; Singh, A.; Atwood, J. L.; Rogers, R. D.; Shakir, R. *J. Am. Chem. Soc.* **1983**, *105*, 302.
(26) Barr, D.; Clegg, W.; Mulvey, R. E.; Snaith, R. *J. Chem. Soc., Chem. Commun.* **1984**, 285.
(27) Fjeldberg, T.; Hitchcock, P. B.; Lappert, M. F.; Thorne, A. J. *J. Chem. Soc., Chem. Commun.* **1984**, 822.

Table 5. Selected Bond Lengths (Å) and Angles (deg) for 9a and 10a,b

	{MeC(N^{i}Pr)$_2$}$_2$AlCl (**9a**)[a]		
Al(1)−N(2)	1.914(2)	Al(1)−N(2A)	1.914(2)
Al(1)−N(1)	2.041(2)	Al(1)−N(1A)	2.041(2)
Al(1)−Cl(1)	2.1609(13)	N(1)−C(4)	1.323(3)
N(1)−C(2)	1.479(3)	N(2)−C(4)	1.341(3)
N(2)−C(7)	1.468(3)	C(4)−C(5)	1.503(3)
N(2)−Al(1)−N(2A)	118.01(12)	N(2)−Al(1)−N(1A)	104.06(8)
N(2A)−Al(1)−N(1A)	67.18(8)	N(2)−Al(1)−N(1)	67.18(8)
N(2A)−Al(1)−N(1)	104.06(8)	N(1A)−Al(1)−N(1)	163.83(12)
N(2)−Al(1)−Cl(1)	121.00(6)	N(2A)−Al(1)−Cl(1)	121.00(6)
N(1A)−Al(1)−Cl(1)	98.08(6)	N(1)−Al(1)−Cl(1)	98.08(6)
C(4)−N(2)−C(2)	121.7(2)	C(4)−N(1)−Al(1)	88.59(13)
C(2)−N(1)−Al(1)	147.6(2)	C(4)−N(2)−C(7)	123.7(2)
C(4)−N(2)−Al(1)	93.59(14)	C(7)−N(2)−Al(1)	140.80(14)
N(1)−C(4)−N(2)	110.6(2)		
	{^{t}BuC(N^{i}Pr)$_2$}$_2$AlCl (**10a**)		
Al(1)−N(1)	1.9173(12)	Al(1)−N(2)	1.9853(12)
Al(1)−N(3)	1.9379(12)	Al(1)−N(4)	1.9911(12)
Al(1)−Cl(1)	2.2018(6)	N(1)−C(7)	1.349(2)
N(1)−C(1)	1.468(2)	N(2)−C(7)	1.338(2)
N(2)−C(4)	1.474(2)	N(3)−C(27)	1.345(2)
N(3)−C(21)	1.473(2)	N(4)−C(27)	1.339(2)
N(4)−C(24)	1.477(2)	C(7)−C(8)	1.547(2)
C(27)−C(28)	1.553(2)		
N(1)−Al(1)−N(3)	110.33(5)	N(1)−Al(1)−N(2)	67.71(5)
N(3)−Al(1)−N(2)	103.70(5)	N(1)−Al(1)−N(4)	107.22(5)
N(3)−Al(1)−N(4)	67.32(5)	N(2)−Al(1)−N(4)	168.10(5)
N(1)−Al(1)−Cl(1)	120.53(4)	N(3)−Al(1)−Cl(1)	129.15(4)
N(2)−Al(1)−Cl(1)	95.45(4)	N(4)−Al(1)−Cl(1)	96.35(4)
C(7)−N(1)−C(1)	128.61(12)	C(7)−N(1)−Al(1)	93.42(8)
C(1)−N(1)−Al(1)	137.84(9)	C(7)−N(2)−C(4)	127.45(12)
C(7)−N(2)−Al(1)	90.79(8)	C(4)−N(2)−Al(1)	136.40(10)
C(27)−N(3)−C(21)	127.24(12)	C(27)−N(3)−Al(1)	93.10(8)
C(21)−N(3)−Al(1)	138.01(10)	C(27)−N(4)−C(24)	125.82(12)
C(27)−N(4)−Al(1)	90.95(8)	C(24)−N(4)−Al(1)	136.44(9)
N(1)−C(7)−N(2)	108.03(11)	N(4)−C(27)−N(3)	108.51(12)
	{^{t}BuC(NCy)$_2$}$_2$AlCl (**10b**), Molecule 1		
Al(1)−N(1)	1.915(2)	Al(1)−N(2)	1.986(2)
Al(1)−N(3)	1.997(2)	Al(1)−N(4)	1.939(2)
Al(1)−Cl(1)	2.2091(11)	N(1)−C(1)	1.350(3)
N(1)−C(11)	1.471(3)	N(2)−C(1)	1.334(3)
N(2)−C(21)	1.468(3)	N(3)−C(6)	1.339(3)
N(3)−C(31)	1.468(3)	N(4)−C(6)	1.351(3)
N(4)−C(41)	1.475(3)	C(1)−C(2)	1.557(4)
C(6)−C(7)	1.551(4)		
N(1)−Al(1)−N(4)	112.55(10)	N(1)−Al(1)−N(2)	67.84(9)
N(4)−Al(1)−N(2)	101.18(10)	N(1)−Al(1)−N(3)	110.29(10)
N(3)−Al(1)−N(4)	67.22(9)	N(2)−Al(1)−N(3)	167.03(10)
N(1)−Al(1)−Cl(1)	115.53(8)	N(4)−Al(1)−Cl(1)	131.91(7)
N(2)−Al(1)−Cl(1)	95.65(7)	N(3)−Al(1)−Cl(1)	96.58(7)
C(1)−N(1)−C(11)	128.2(2)	C(1)−N(1)−Al(1)	93.1(2)
C(11)−N(1)−Al(1)	138.6(2)	C(1)−N(2)−C(21)	130.0(2)
C(1)−N(2)−Al(1)	90.5(2)	C(21)−N(2)−Al(1)	137.1(2)
C(6)−N(3)−C(31)	126.8(2)	C(6)−N(3)−Al(1)	91.2(2)
C(31)−N(3)−Al(1)	138.0(2)	C(6)−N(4)−C(41)	125.1(2)
C(6)−N(4)−Al(1)	93.3(2)	C(41)−N(4)−Al(1)	136.7(2)
N(1)−C(1)−N(2)	108.4(2)	N(3)−C(6)−N(4)	108.3(2)

[a] Symmetry transformations used to generate equivalent atoms: $-x, y, -z + 3/2$.

arrangement, including {MeC$_6$H$_4$C(NSiMe$_3$)$_2$Li(THF)$_2$}$_2$, Li[CPh(NPh)$_2$]·tmen, and {Li[MeC(NPh)$_2$]·hmpa}$_2$.[28]

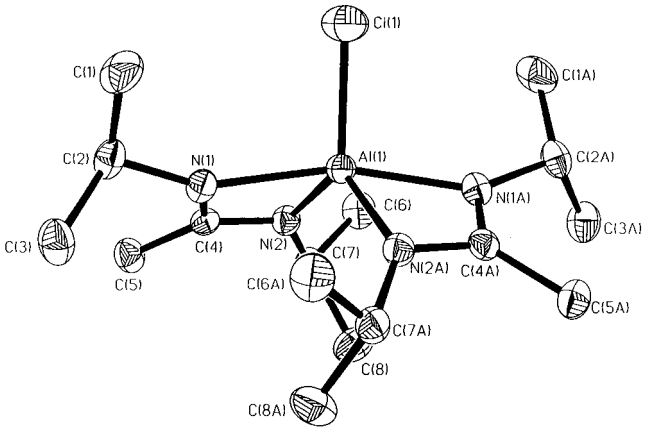

Figure 8. Molecular structure of {MeC(N^{i}Pr)$_2$}$_2$AlCl (**9a**, H-atoms omitted).

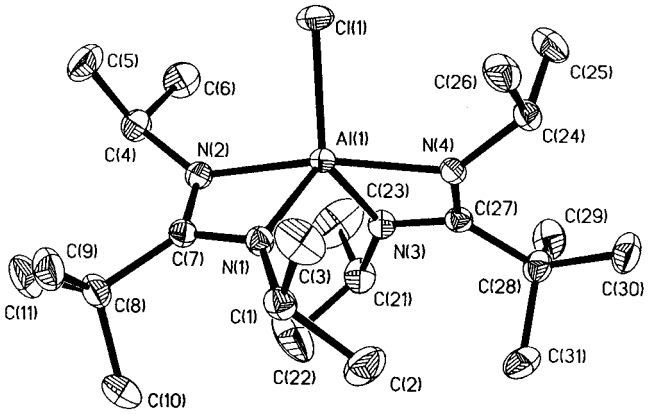

Figure 9. Molecular structure of {^{t}BuC(N^{i}Pr)$_2$}$_2$AlCl (**10a**, H-atoms omitted).

Discussion

As illustrated in Chart 2, in an idealized amidinate structure with 120° bond angles at the C and N centers, the nitrogen sp^2 donor orbitals project in parallel directions and a bridging bonding mode should be favored (**C**). Increasing the R−C−N and C−N−R′ angles will cause the nitrogen σ donor orbitals to project more toward the center of the amidinate "mouth" and should favor a chelating bonding mode (**D**). As noted in the introduction, it was shown previously that [{MeC(NMe$_2$)$_2$}AlMe$_2$]$_2$ adopts a dinuclear structure with bridging amidinate ligands,[7] while {PhC(NSiMe$_3$)$_2$}AlCl$_2$,[3] {MeC(NSiMe$_3$)$_2$}AlMe$_2$,[1,2] and {MeC(N^{i}Pr)$_2$}AlMe$_2$[1] adopt monomeric structures with chelating amidinate ligands. These differences may be rationalized in terms of steric interactions between the amidinate substituents. For the bulkier amidinate ligands, steric crowding between the C−*R* and the N−*R*′ groups increases the R−C−N and C−N−R′ angles, favoring monomeric structures. In the present work, we have found that {RC(NR′)$_2$}AlX$_2$ (X = Cl, Me, CH$_2$Ph, and CH$_2$CMe$_3$) complexes containing the bulky amidinate ligands MeC(N^{i}Pr)$_2^-$, MeC(NCy)$_2^-$, ^{t}BuC(N^{i}Pr)$_2^-$, ^{t}BuC(NCy)$_2^-$, and ^{t}BuC(NSiMe$_3$)$_2^-$ are all monomeric.

Steric interactions between the C−*R* and the N−*R*′ groups also influence the steric environment at the Al center. In particular, increasing the C−N−R′ angle causes the N−*R*′ substituents to project more toward the metal center, in effect increasing the cone angle of the amidinate ligand. This effect was invoked by

(28) (a) Stalke, D.; Wedler, M.; Edelmann, F. T. *J. Organomet. Chem.* **1992**, *431*, C1. (b) Gebauer, T.; Dehnicke, K.; Goesmann, H.; Fenske, D. *Z. Naturforsch.* **1994**, *49b*, 1444. (c) Westerhausen, M.; Schwarz, W. *Z. Anorg. Allg. Chem.* **1993**, 1053. (d) Eisen, M. S.; Kapon, M. *J. Chem. Soc., Dalton Trans.* **1994**, 3507. (e) Cragg-Hine, I.; Davidson, M. G.; Mair, F. S.; Raithby, P. R.; Snaith, R. *J. Chem. Soc., Dalton Trans.* **1993**, 2423. (f) Barker, J.; Barr, D.; Barnett, N. D. R.; Clegg, W.; Cragg-Hine, I.; Davidson, M. G.; Davies, R. P.; Hodgson, S. M.; Howard, J. A. K.; Kilner, M.; Lehmann, C. W.; Lopez-Solera, I.; Mulvey, R. E.; Raithby, P. R.; Snaith, R. *J. Chem. Soc., Dalton Trans.* **1997**, 951. (g) Hagadorn, J. R.; Arnold, J. *Inorg. Chem.* **1997**, *36*, 132.

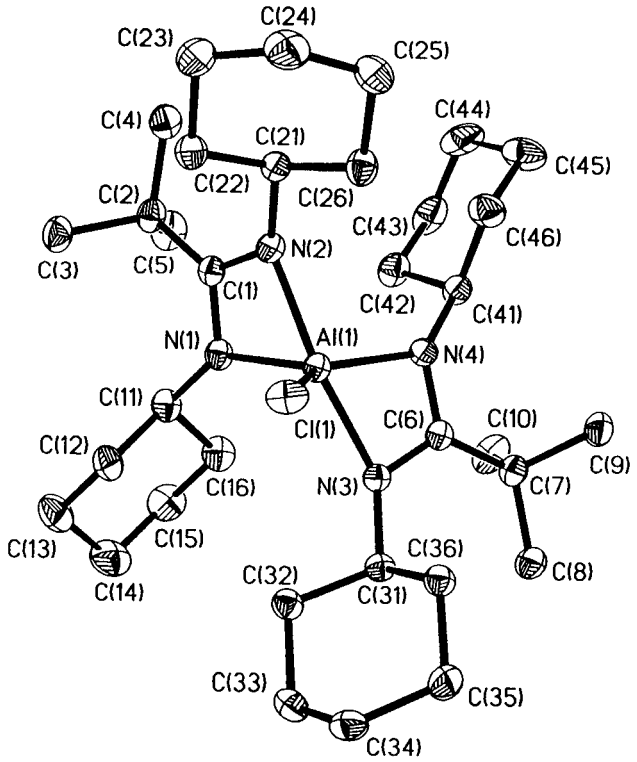

Figure 10. Molecular structure of $\{^t\text{BuC(NCy)}_2\}_2\text{AlCl}$ (**10b**, H-atoms omitted).

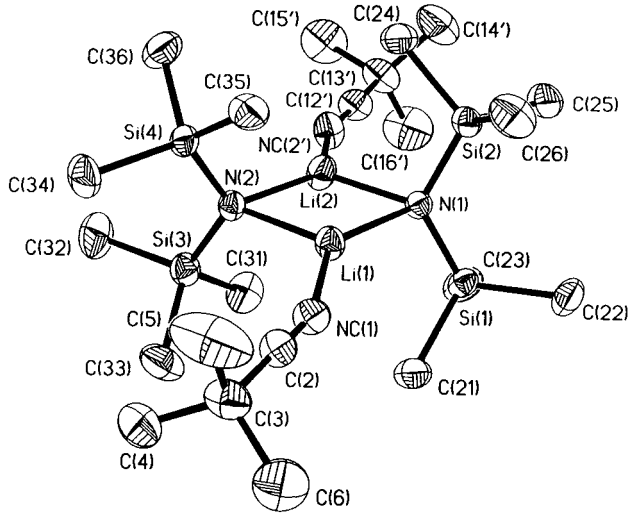

Figure 11. Molecular structure of $[\text{Li}(^t\text{BuCN})\{\mu\text{-N(SiMe}_3)_2\}]_2$ (**3d**, H-atoms omitted).

Chart 1

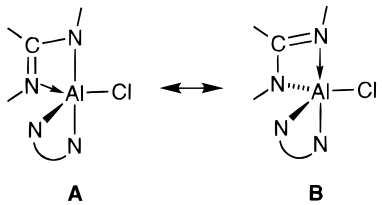

Richeson to explain the increased fluxionality observed for $\{\text{HC(NCy)}_2\}_2\text{SnCl}_2$ compared to $\{\text{MeC(NCy)}_2\}_2\text{SnCl}_2$ and $\{^t\text{Bu(NSiMe}_3)_2\}_2\text{SnCl}_2$,[9] and by Gambarotta to rationalize structural trends in transition metal amidinate compounds.[29] In the present work, we have found that the R′−N−Al angles in $\{^t\text{BuC(NR′)}_2\}\text{AlX}_2$ compounds are ca. 8° smaller than those in $\{\text{MeC(NR′)}_2\}\text{AlX}_2$ compounds, which implies that the cone angles of the ^{t}Bu−amidinate ligands are larger than those of analogous acetamidinate ligands. The resulting difference in steric crowding at the Al center strongly influences the chemistry of related $\{\text{RC(NR′)}_2\}\text{Al(R)}^+$ cations.[13] For example, acetamidinate complex **1a** reacts with 0.5 equiv of $\text{B(C}_6\text{F}_5)_3$ to yield 0.5 equiv of the dinuclear cation $[\{\text{MeC(N}^i\text{Pr)}_2\}\text{AlMe}]_2(\mu\text{-Me})^+$ (**11**, as the $\text{MeB(C}_6\text{F}_5)_3^-$ salt), via generation of $\{\text{MeC(N}^i\text{Pr)}_2\}$-$\text{AlMe}^+$, which is trapped by **1a** (eq 2). In contrast, the

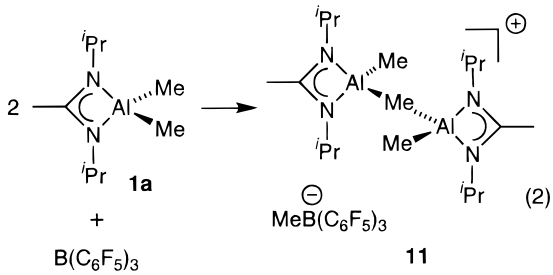

^{t}Bu-amidinate analogue **6a** reacts with 1 equiv of $\text{B(C}_6\text{F}_5)_3$ to yield $\{^t\text{BuC(N}^i\text{Pr)}_2\}\text{Al(Me)}(\mu\text{-Me})\text{B(C}_6\text{F}_5)_3$ (**12**, eq 3). In this case, the increased crowding in $\{^t\text{BuC-(N}^i\text{Pr)}_2\}\text{AlMe}^+$ and **6a** inhibits formation of a dinuclear cation.

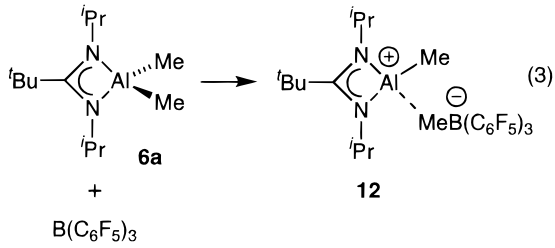

In the chelated $\{\text{RC(NR′)}_2\}\text{M}$ structures, the N−C−N angle is reduced by ca. 11° from the ideal trigonal planar value of 120° and the N−M−N angle is highly acute (ca. 70°), indicating that considerable ring strain must be present. Increasing the M−N distances by, for example, employing larger metals or by reducing the Lewis acidity of the metal by incorporating more strongly electron-donating ligands should decrease the N−M−N angle further and may disfavor the chelating bonding mode. Thus, the combination of a sterically undemanding C−*H* unit and long M−N bonds may explain why $[\{\text{HC(NCy)}_2\}\text{InMe}]_2$ adopts a dinuclear structure.[8] In the present work, we have found that the Al−N bonds in $\{\text{RC(NR′)}_2\}\text{AlMe}_2$ complexes are ca. 0.06 Å longer than those in analogous $\{\text{RC(NR′)}_2\}\text{AlCl}_2$ complexes, presumably reflecting the stronger electron-donating ability of Me^- versus Cl^-.[30] However, this difference in bond length does not cause a difference in amidinate bonding mode.

Experimental Section

General Procedures. All manipulations were performed on a high-vacuum line or in a glovebox under a purified N_2 atmosphere. Solvents were distilled from Na/benzophenone

(29) (a) Hao, S.; Gambarotta, S.; Bensimon, C.; Edema, J. J. H. *Inorg. Chim. Acta* **1993**, *213*, 65. (b) Hao, S.; Berno, P.; Minhas, R. K.; Gambarotta, S. *Inorg. Chim. Acta* **1996**, *244*, 37. (c) Hao, S.; Feghali, K.; Gambarotta, S. *Inorg. Chem.* **1997**, *36*, 1745.

(30) Differences in the hybridization of the Al orbitals may also influence the Al−N bond lengths. See ref 17.

Table 6. Summary of Crystal Data for Compound 3d

complex	**3d**
formula	$C_{22}H_{54}Li_2N_4Si_4$
fw	500.93
cryst size, mm	0.45 × 0.38 × 0.27
color/shape	colorless/prism
d (calcd), Mg/m^3	0.950
cryst syst	triclinic
space group	$P\bar{1}$
a, Å	13.125(1)
b, Å	15.033(1)
c, Å	9.234(1)
α, deg	100.04(1)
β, deg	100.74(1)
γ, deg	94.29(1)
V, Å^3	1751.7(3)
Z	2
T, K	213(2)
diffractometer	Enraf-Nonius CAD4
radiation, *λ*, Å	Mo Kα, 0.710 73
2*θ* range, deg	4.0 < 2*θ* < 55.0
data colld: *h*;*k*;*l*	±16; ±19; −11,4
no. of reflns	9912
no. of unique reflns	7873
R_{int}	0.0134
no. of obsd reflns	$I > 2\sigma(I)$, 6186
μ, mm^{-1}	0.184
transmission range, %	98−100
structure solution	direct methods[a]
GOF on F^2	1.079
R Indices ($I > 2\sigma(I)$)	R1 = 0.0413,[b] wR2 = 0.1102[c]
R Indices (all data)	R1 = 0.0600,[b] wR2 = 0.1280[c]
max resid density (e/Å3)	0.37

[a] *MULTAN*, *Multan80*; University of York: York, England. [b] $R1 = \sum||F_o| - |F_c||/\sum|F_o|$. [c] $wR2 = [\sum[w(F_o^2 - F_c^2)^2]/\sum[w(F_o^2)^2]]^{1/2}$, where $w = 1/\sigma^2(F_o^2) + (aP)^2 + bP$.

Table 7. Selected Bond Lengths (Å) and Angles (deg) for 3d

Li(1)−N(1)	2.026(3)	Li(1)−N(2)	2.036(3)
Li(2)−N(1)	2.032(3)	Li(2)−N(2)	2.021(3)
Li(1)−NC(1)	2.058(3)	Li(2)−NC(2)	2.067(4)
Li(1)−Li(2)	2.459(4)	N(1)−Si(1)	1.7011(13)
N(1)−Si(2)	1.6984(14)	N(2)−Si(3)	1.699(2)
N(2)−Si(4)	1.6987(14)		
N(1)−Li(1)−N(2)	105.19(13)	N(1)−Li(2)−N(2)	105.53(14)
Li(1)−N(1)−Li(2)	74.60(12)	Li(1)−N(2)−Li(2)	74.62(12)
N(1)−Li(1)−NC(1)	138.7(3)	N(2)−Li(1)−NC(1)	115.9(3)
N(1)−Li(2)−NC(2)	112.0(5)	N(2)−Li(2)−NC(2)	142.5(5)
Li(1)−N(1)−Si(1)	106.11(10)	Li(1)−N(1)−Si(2)	120.54(11)
Li(2)−N(1)−Si(1)	118.23(12)	Li(2)−N(1)−Si(2)	104.61(11)
Li(1)−N(2)−Si(3)	117.30(11)	Li(1)−N(2)−Si(4)	105.88(11)
Li(2)−N(2)−Si(3)	106.00(12)	Li(2)−N(2)−Si(4)	120.10(12)
Si(1)−N(1)−Si(2)	123.20(7)	Si(3)−N(2)−Si(4)	123.29(8)
Li(1)−NC(1)−C(2)	159.8(9)	NC(1)−C(2)−C(3)	174.2(7)
Li(2)−NC(2)−C(12)	168(2)	NC(2)−C(12)−C(13)	169.9(11)

ketyl, except for chlorinated solvents, which were distilled from activated molecular sieves (3 Å) or CaH_2. All other chemicals were purchased from Aldrich and used as received.

NMR spectra were recorded on a Bruker AMX 360 spectrometer in sealed or Teflon-valved tubes at ambient-probe temperature unless otherwise indicated. ^{1}H and ^{13}C chemical shifts are reported versus $SiMe_4$ and were determined by reference to the residual ^{1}H and ^{13}C solvent peaks. Coupling constants are reported in hertz. Mass spectra were obtained using the direct insertion probe method on a VG Analytical Trio I instrument operating at 70 eV. Elemental analyses were performed by Desert Analytics Laboratory. IR spectra were recorded on a Mattson CYGNUS 25, over 16 scans at 4 cm^{-1} resolution. IR and mass spectral data appear in the Supporting Information.

{MeC(N^{i}Pr)$_2$}AlMe$_2$ (1a). A solution of 1,3-diisopropylcarbodiimide (2.00 g, 10.7 mmol) in hexane (25 mL) was added dropwise to a rapidly stirring solution of $AlMe_3$ (1.06 mL, 11.0 mmol) in hexane (10 mL). The reaction mixture was stirred at room temperature for 18 h, and the volatiles were removed under vacuum, affording pure {MeC(N^{i}Pr)$_2$}AlMe$_2$ as a pale yellow liquid (2.30 g, 71%). ^{1}H NMR (CD_2Cl_2): *δ* 3.50 (sept, $^3J_{HH}$ = 6.3, 2H, C*H*Me$_2$), 1.94 (s, 3H, C*Me*), 1.05 (d, $^3J_{HH}$ = 6.1, 12H, CH*Me*$_2$), −0.82 (s, 6H, Al*Me*$_2$). ^{13}C NMR (CD_2Cl_2): *δ* 172.5 (s, *C*Me), 45.3 (d, $^1J_{CH}$ = 132.2, *C*HMe$_2$), 25.3 (q, $^1J_{CH}$ = 125.6, CH*Me*$_2$), 11.1 (q, $^1J_{CH}$ = 128.3, C*Me*), −9.94 (br q, $^1J_{CH}$ = 114.1, Al*Me*$_2$). Anal. Calcd for $C_{10}H_{23}AlN_2$: C, 60.57; H, 11.69; N, 14.13. Found: C, 60.41; H, 11.96; N, 14.50.

{MeC(NCy)$_2$}AlMe$_2$ (1b). This compound was prepared by the procedure described for **1a**, using 5.00 g of 1,3-dicyclohexylcarbodiimide (24.2 mmol) in 40 mL of hexane and 2.40 mL of $AlMe_3$ (25.0 mmol) in 15 mL of hexane. After 15 h, the volatiles were removed under vacuum, yielding a pale yellow liquid that crystallized upon standing to afford {MeC(NCy)$_2$}-AlMe$_2$ as off-white crystals (6.49 g, 93%). ^{1}H NMR (CD_2Cl_2): *δ* 3.10 (m, 2H, *Cy*), 1.92 (s, 3H, C*Me*), 1.69 (m, 8H, *Cy*), 1.56 (m, 2H, *Cy*), 1.35−1.06 (m, 8H + 2H, *Cy*), −0.82 (s, 6H, Al*Me*$_2$). ^{13}C NMR (CD_2Cl_2): *δ* 172.4 (s, *C*Me), 53.0 (d, $^1J_{CH}$ = 131.4, Cy−*C*$_1$), 36.0 (t, $^1J_{CH}$ = 126.5, *Cy*), 26.1 (t, $^1J_{CH}$ = 125.8, *Cy*), 25.4 (t, $^1J_{CH}$ = 126.9, *Cy*), 11.2 (q, $^1J_{CH}$ = 128.0, C*Me*), −9.78 (br q, $^1J_{CH}$ = 112.6, Al*Me*$_2$). Anal. Calcd for $C_{16}H_{31}AlN_2$: C, 69.02; H, 11.22; N, 10.06. Found: C, 68.88; H, 10.44; N, 10.15.

Li[MeC(N^{i}Pr)$_2$] (2a). A solution of 1,3-diisopropylcarbodiimide (5.00 g, 39.6 mmol) in Et_2O (50 mL) was cooled to 0 °C. MeLi (28.3 mL of a 1.4 M solution in Et_2O, 39.6 mmol) was added dropwise, and the mixture was allowed to warm to room temperature. After 30 min, the solvent was removed under vacuum, affording an off-white solid, which was washed with pentane and dried under vacuum (5.31 g, 90%). ^{1}H NMR (THF-d_8): *δ* 3.46 (sept, $^3J_{HH}$ = 5.2, 2H, C*H*Me$_2$), 1.78 (s, 3H, C*Me*), 0.99 (d, $^3J_{HH}$ = 6.2, CH*Me*$_2$). ^{13}C NMR (THF-d_8): *δ* 169.2 (s, *C*Me), 47.9 (d, $^1J_{CH}$ = 122.7, *C*HMe$_2$), 27.3 (q, $^1J_{CH}$ = 123.5, CH*Me*$_2$), 10.8 (q, $^1J_{CH}$ = 124.8, C*Me*).

Scheme 3

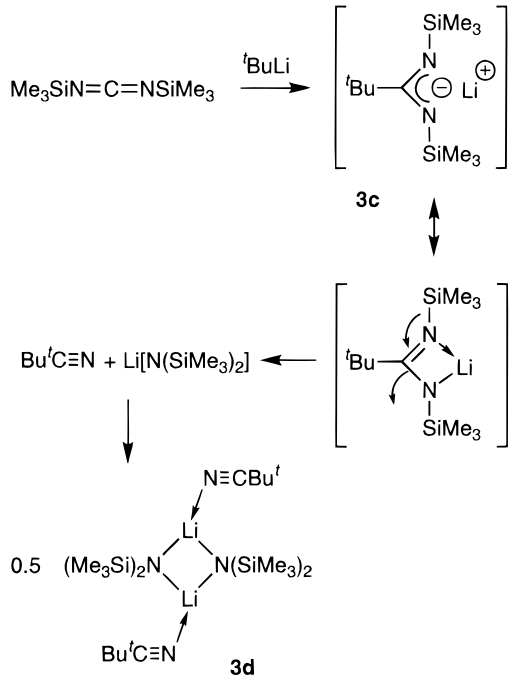

Chart 2

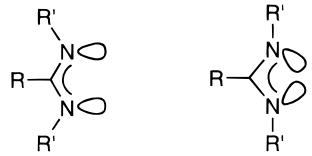

Li[^{t}BuC(N^{i}Pr)$_2$] (3a). This compound was prepared by the procedure described for **2a**, using 5.00 g of 1,3-diisopropylcarbodiimide (39.6 mmol) and 23.3 mL of ^{t}BuLi (1.7 M solution in pentane, 39.6 mmol). After 30 min, the solvent was removed under vacuum, affording a yellow oily solid, which was dried under vacuum (18 h, 23 °C) to give a pale yellow solid. Trituration with hexane gave Li[^{t}BuC(N^{i}Pr)$_2$] as an off-white powder (4.56 g, 61%). ^{1}H NMR (THF-d_8): δ 3.84 (sept, $^3J_{HH}$ = 5.7, 2H, C*H*Me$_2$), 1.13 (s, 9H, C*Me*$_3$), 0.96 (d, $^3J_{HH}$ = 6.1, 12H, CH*Me*$_2$). ^{13}C NMR (THF-d_8): δ 168.5 (s, *C*CMe$_3$), 46.6 (d, $^1J_{CH}$ = 122.3, *C*HMe$_2$), 39.4 (s, *C*Me$_3$), 31.0 (q, $^1J_{CH}$ = 116.1, CH*Me*$_2$), 26.3 (q, $^1J_{CH}$ = 116.1, C*Me*$_3$).

Li[^{t}BuC(NCy)$_2$] (3b). This compound was prepared by the procedure described for **3a**, using 5.00 g of 1,3-dicyclohexylcarbodiimide (24.2 mmol) and 14.3 mL of ^{t}BuLi (1.7 M solution in pentane, 24.2 mmol). Trituration with hexane gave Li[^{t}BuC(NCy)$_2$] as a pale yellow powder (4.91 g, 75%). ^{1}H NMR (THF-d_8): δ 3.50 (m, 2H, *Cy*), 1.81−0.93 (m, 20H, *Cy*), 1.10 (s, 9H, C*Me*$_3$). ^{13}C NMR (THF-d_8): δ 168.3 (s, *C*CMe$_3$), 55.9 (d, $^1J_{CH}$ = 119.8, Cy−*C*$_1$), 39.5 (s, *C*Me$_3$), 37.7 (t, $^1J_{CH}$ = 118.9, *Cy*), 31.1 (q, $^1J_{CH}$ = 117.7, C*Me*$_3$), 28.2 (t, partially obscured, *Cy*), 26.8 (t, $^1J_{CH}$ = 119.4, *Cy*).

[Li(^{t}BuCN){μ-N(SiMe$_3$)$_2$}]$_2$ (3d). This compound was prepared by the procedure described for **3a**, using 3.00 g of 1,3-bis(trimethylsilyl)carbodiimide (16.1 mmol) and 9.50 mL of ^{t}BuLi (1.7 M solution in pentane, 16.1 mmol). Recrystallization from pentane yielded [Li(^{t}BuCN){μ-N(SiMe$_3$)$_2$}]$_2$ as white crystals (2.74 g, 68%). ^{1}H NMR (THF-d_8): δ 1.29 (s, 18H, C*Me*$_3$), −0.11 (br s, 36H, Si*Me*$_3$). ^{13}C NMR (THF-d_8): δ 125.8 (s, *C*≡N), 28.7 (q, $^1J_{CH}$ = 125.8, C*Me*$_3$), 28.8 (s, *C*Me$_3$), 6.1 (q, $^1J_{CH}$ = 123.9, Si*Me*$_3$).

{**MeC(N^{i}Pr)$_2$**}**AlCl$_2$ (4a).** A solution of AlCl$_3$ (1.80 g, 13.5 mmol) in Et$_2$O (20 mL) at −78 °C was added dropwise to a slurry of Li[MeC(N^{i}Pr)$_2$] (2.00 g, 13.5 mmol) in Et$_2$O (50 mL) at −78 °C. The reaction mixture was allowed to warm to room temperature and was stirred for 16 h, resulting in a slurry of a white solid in a yellow solution. The volatiles were removed under vacuum, the crude product was extracted with pentane, and the extract was concentrated to dryness under vacuum. Pure samples of {MeC(N^{i}Pr)$_2$}AlCl$_2$ were obtained by sublimation (50 °C, 0.005 mmHg) (1.71 g, 52%). ^{1}H NMR (CD$_2$Cl$_2$): δ 3.56 (br sept, $^3J_{HH}$ = 6.1, 2H, C*H*Me$_2$), 2.09 (s, 3H, C*Me*), 1.14 (d, $^3J_{HH}$ = 6.4, CH*Me*$_2$). ^{13}C NMR (CD$_2$Cl$_2$): δ 178.2 (s, *C*Me), 45.6 (d, $^1J_{CH}$ = 134.9, *C*HMe$_2$), 24.8 (q, $^1J_{CH}$ = 127.1, CH*Me*$_2$), 12.0 (q, $^1J_{CH}$ = 129.7, C*Me*). Anal. Calcd for C$_8$H$_{17}$AlCl$_2$N$_2$: C, 40.18; H, 7.17; N, 11.71. Found: C, 40.48; H, 7.49; N, 11.50.

{**^{t}BuC(N^{i}Pr)$_2$**}**AlCl$_2$ (5a).** This compound was prepared by the procedure described for **4a**, using 1.40 g of AlCl$_3$ (10.5 mmol) and 2.00 g of Li[^{t}BuC(N^{i}Pr)$_2$] (10.5 mmol). The pentane extract was concentrated and cooled to 0 °C to afford {^{t}BuC(N^{i}Pr)$_2$}AlCl$_2$ as white crystals, which were collected by filtration (2.01 g, 68%). ^{1}H NMR (CD$_2$Cl$_2$): δ 4.12 (br sept, $^3J_{HH}$ = 5.9, 2H, C*H*Me$_2$), 1.43 (s, 9H, C*Me*$_3$), 1.18 (d, $^3J_{HH}$ = 6.2, 12H, CH*Me*$_2$). ^{13}C NMR (CD$_2$Cl$_2$): δ 184.3 (s, *C*CMe$_3$), 46.6 (d, $^1J_{CH}$ = 135.7, *C*HMe$_2$), 40.1 (s, *C*Me$_3$), 29.2 (q, $^1J_{CH}$ = 125.7, C*Me*$_3$), 25.9 (q, $^1J_{CH}$ = 124.1, CH*Me*$_2$). Anal. Calcd for C$_{11}$H$_{23}$AlCl$_2$N$_2$: C, 46.98; H, 8.24; N, 9.96. Found: C, 46.84; H, 8.12; N, 9.85.

{**^{t}BuC(NCy)$_2$**}**AlCl$_2$ (5b).** This compound was prepared by the procedure described for **4a**, using 1.0 g of AlCl$_3$ (7.4 mmol) in 25 mL of Et$_2$O and 2.0 g of Li[^{t}BuC(NCy)$_2$] (7.4 mmol) in 50 mL of Et$_2$O. The product was extracted from the LiCl with toluene. Concentration and cooling of the toluene extract to 0 °C afforded {^{t}BuC(NCy)$_2$}AlCl$_2$ as colorless crystals, which were collected by filtration (1.84 g, 69%). ^{1}H NMR (CD$_2$Cl$_2$): δ 3.62 (br m, 2H, *Cy*), 1.41 (s, 9H, C*Me*$_3$), 1.91−1.71 (m, 4H, *Cy*), 1.62 (m, 2H, *Cy*), 1.30−1.09 (m, 8H + 2H, *Cy*). ^{13}C NMR (CD$_2$Cl$_2$): δ 184.4 (s, *C*CMe$_3$), 54.6 (d, $^1J_{CH}$ = 138.7, Cy−*C*$_1$), 40.1 (s, *C*Me$_3$), 36.9 (t, $^1J_{CH}$ = 127.9, *Cy*), 29.3 (q, $^1J_{CH}$ = 127.7, C*Me*$_3$), 25.7 (t, $^1J_{CH}$ = 125.7, *Cy*), 25.6 (t, $^1J_{CH}$ = 125.7, *Cy*). Anal. Calcd for C$_{17}$H$_{31}$AlCl$_2$N$_2$: C, 56.51; H, 8.65; N, 7.75. Found: C, 56.22; H, 8.70; N, 7.67.

{**^{t}BuC(NSiMe$_3$)$_2$**}**AlCl$_2$ (5c).** A solution of 1,3-bis(trimethylsilyl)carbodiimide (1.0 g, 5.4 mmol) in Et$_2$O (35 mL) was cooled to 0 °C. ^{t}BuLi (3.2 mL of a 1.7 M solution in hexanes, 5.4 mmol) was added slowly by syringe. The resulting mixture was allowed to warm to room temperature and was stirred for 30 min. The mixture was cooled to −78 °C, and a solution of AlCl$_3$ (0.71 g, 5.4 mmol) in Et$_2$O (15 mL) was added. The resulting solution was allowed to warm to room temperature over 5 h. After a further 16 h, the volatiles were removed and the product was extracted from the LiCl with pentane. The pentane extract was concentrated and cooled to −30 °C to afford {^{t}BuC(NSiMe$_3$)$_2$}AlCl$_2$ as white crystals, which were isolated by filtration (1.02 g, 56% based on AlCl$_3$). ^{1}H NMR (CD$_2$Cl$_2$): δ 1.33 (s, 9H, C*Me*$_3$), 0.34 (s, 18H, Si*Me*$_3$). ^{13}C NMR (CD$_2$Cl$_2$): δ 195.4 (s, *C*CMe$_3$), 41.0 (s, *C*Me$_3$), 29.5 (q, $^1J_{CH}$ = 121.7, C*Me*$_3$), 3.3 (q, $^1J_{CH}$ = 113.9, Si*Me*$_3$). Anal. Calcd for C$_{11}$H$_{27}$AlCl$_2$N$_2$Si$_2$: C, 38.70; H, 7.97; N, 8.21. Found: C, 38.82; H, 8.10; N, 8.17.

{**^{t}BuC(N^{i}Pr)$_2$**}**AlMe$_2$ (6a).** This compound was prepared by the procedure described for **4a**, using 0.25 mL of AlMe$_2$Cl (2.7 mmol) in 25 mL of Et$_2$O and 0.50 g of Li[^{t}BuC(N^{i}Pr)$_2$] (2.6 mmol) in 30 mL of Et$_2$O. The extract was evaporated to dryness under vacuum, yielding {^{t}BuC(N^{i}Pr)$_2$}AlMe$_2$ as a pale yellow solid (0.57 g, 87%). Analytically pure samples of {^{t}BuC(N^{i}Pr)$_2$}AlMe$_2$ were obtained by sublimation (50 °C, 0.005 mmHg). ^{1}H NMR (CD$_2$Cl$_2$): δ 4.07 (sept, $^3J_{HH}$ = 6.2, 2H, C*H*Me$_2$), 1.38 (s, 9H, C*Me*$_3$), 1.06 (d, $^3J_{HH}$ = 6.1, 12H, CH*Me*$_2$), −0.81 (s, 6H, Al*Me*$_2$). ^{13}C NMR (CD$_2$Cl$_2$): δ 178.4 (s, *C*CMe$_3$), 45.8 (d, $^1J_{CH}$ = 135.3, *C*HMe$_2$), 40.0 (s, *C*Me$_3$), 29.7 (q, $^1J_{CH}$ = 127.0, CH*Me*$_2$), 26.3 (q, $^1J_{CH}$ = 125.5, C*Me*$_3$), −9.06 (br q, $^1J_{CH}$ = 105.4, Al*Me*$_2$). Anal. Calcd for C$_{13}$H$_{29}$AlN$_2$: C, 64.96; H, 12.16; N, 11.65. Found: C, 64.46; H, 11.90; N, 11.90.

{**^{t}BuC(NCy)$_2$**}**AlMe$_2$ (6b).** This compound was prepared by the procedure described for **4a**, using 0.71 mL of AlMe$_2$Cl (7.7 mmol) in 30 mL of Et$_2$O and 2.0 g of Li[^{t}BuC(NCy)$_2$] (7.4 mmol) in 40 mL of Et$_2$O. Concentration of the pentane extract afforded {^{t}BuC(NCy)$_2$}AlMe$_2$ (2.00 g, 83%) as large colorless crystals, which were collected by filtration. ^{1}H NMR (CD$_2$Cl$_2$): δ 3.56 (m, 2H, *Cy*), 1.80−1.69 (m, 8H, *Cy*), 1.61−1.57 (m, 2H, *Cy*), 1.36 (s, 9H, C*Me*$_3$), 1.27−1.03 (m, 8H + 2H, *Cy*), −0.83 (s, 6H, Al*Me*$_2$). ^{13}C NMR (CD$_2$Cl$_2$): δ 178.5 (s, *C*CMe$_3$), 54.2 (d, $^1J_{CH}$ = 125.9, Cy−*C*$_1$), 39.9 (s, *C*Me$_3$), 37.3 (t, $^1J_{CH}$ = 119.3, *Cy*), 29.7 (q, $^1J_{CH}$ = 117.3, C*Me*$_3$), 26.1 (t, $^1J_{CH}$ = 119.3, *Cy*), 26.0 (t, $^1J_{CH}$ = 119.3, *Cy*), −9.1 (br q, $^1J_{CH}$ = 103.9, Al*Me*$_2$). Anal. Calcd for C$_{19}$H$_{37}$AlN$_2$: C, 71.20; H, 11.64; N, 8.74. Found: C, 71.18; H, 11.88; N, 8.73.

{**^{t}BuC(NSiMe$_3$)$_2$**}**AlMe$_2$ (6c).** This compound was prepared by the procedure described for **5c**, using 2.00 mL of 1,3-bis(trimethylsilyl)carbodiimide (10.7 mmol) in 50 mL of Et$_2$O, 6.30 mL of ^{t}BuLi (1.7 M solution in hexanes, 10.7 mmol) and 1.00 mL of AlMe$_2$Cl (10.7 mmol) in 15 mL of Et$_2$O. The yellow pentane extract was taken to dryness under vacuum, yielding a yellow waxy solid. Pure samples of {^{t}BuC(NSiMe$_3$)$_2$}AlMe$_2$ were obtained by sublimation (50 °C, 0.005 mmHg) (2.16 g, 67% based on AlMe$_2$Cl). ^{1}H NMR (CD$_2$Cl$_2$): δ 1.27 (s, 9H, C*Me*$_3$), 0.23 (s, 18H, Si*Me*$_3$), −0.79 (s, 6H, Al*Me*$_2$). ^{13}C NMR (CD$_2$Cl$_2$): δ 189.5 (s, *C*CMe$_3$), 40.9 (s, *C*Me$_3$), 29.6 (q, $^1J_{CH}$ = 126.7, C*Me*$_3$), 3.4 (q, $^1J_{CH}$ = 109.3, Si*Me*$_3$), −9.4 (br q, $^1J_{CH}$ = 108.4, Al*Me*$_2$). Anal. Calcd for C$_{13}$H$_{33}$AlSi$_2$N$_2$: C, 51.95; H, 11.07; N, 9.32. Found: C, 51.90; H, 11.29; N, 9.28.

{**^{t}BuC(N^{i}Pr)$_2$**}**Al(CH$_2$Ph)$_2$ (7a).** A solution of {^{t}BuC(N^{i}Pr)$_2$}AlCl$_2$ (0.50 g, 1.8 mmol) in Et$_2$O (25 mL) was cooled to −78 °C, and PhCH$_2$MgCl (3.6 mL of a 1.0 M solution in Et$_2$O, 3.6 mmol) was added dropwise. The reaction mixture was allowed to warm to room temperature and was stirred for 15 h. The volatiles were removed under vacuum, and the residue was extracted with pentane. The extract was evaporated to dryness under vacuum, affording pure {^{t}BuC(N^{i}Pr)$_2$}-Al(CH$_2$Ph)$_2$ as a viscous oil (0.55 g, 79%) that solidified after storage at −40 °C. ^{1}H NMR (CD$_2$Cl$_2$): δ 7.11 (t, $^3J_{HH}$ = 7.6, 4H, *m*-Ph), 7.02 (d, $^3J_{HH}$ = 6.9, 4H, *o*-Ph), 6.88 (t, $^3J_{HH}$ = 7.3, 2H, *p*-Ph), 4.00 (sept, $^3J_{HH}$ = 6.2, 2H, C*H*Me$_2$), 1.75 (s, 4H,

CH_2Ph), 1.34 (s, 9H, CMe_3), 0.94 (d, $^3J_{HH}$ = 6.2, 12H, CHMe_2). ^{13}C NMR (CD_2Cl_2): δ 180.8 (s, *C*CMe$_3$), 146.8 (s, *ipso*-Ph), 128.2 (d, $^1J_{CH}$ = 155.8, *o*- or *m*-Ph), 127.5 (d, $^1J_{CH}$ = 149.4, *o*- or *m*-Ph), 121.7 (d, $^1J_{CH}$ = 148.5, *p*-Ph), 45.6 (d, $^1J_{CH}$ = 128.9, *C*HMe$_2$), 40.1 (s, *C*Me$_3$), 29.6 (q, $^1J_{CH}$ = 119.0, C*Me*$_3$), 26.3 (q, $^1J_{CH}$ = 116.4, CH*Me*$_2$), 21.4 (br t, $^1J_{CH}$ = 108.9, *C*H$_2$Ph).

{^{t}BuC(NCy)$_2$}Al(CH$_2$Ph)$_2$ (7b). This compound was prepared by the procedure described for **7a**, using 0.50 g of {^{t}BuC(NCy)$_2$}AlCl$_2$ (1.4 mmol) in 20 mL of Et$_2$O and 2.8 mL of PhCH$_2$MgCl (1.0 M solution in Et$_2$O, 2.8 mmol). The extract was evaporated under vacuum, affording pure {^{t}BuC(NCy)$_2$}Al(CH$_2$Ph)$_2$ as a viscous white oil (0.57 g, 87%). ^{1}H NMR (CD_2Cl_2): δ 7.08 (t, $^3J_{HH}$ = 7.6, 4H, *m*-Ph), 6.98 (d, $^3J_{HH}$ = 6.9, 4H, *o*-Ph), 6.84 (t, $^3J_{HH}$ = 7.3, 2H, *p*-Ph), 3.44 (m, 2H, *Cy*), 1.69 (s, 4H, C*H*$_2$Ph), 1.63−1.51 (m, 4H + 2H, *Cy*), 1.27 (s, 9H, C*Me*$_3$), 1.21−0.78 (m, 14H, *Cy*). ^{13}C NMR (CD_2Cl_2): δ 180.8 (s, *C*CMe$_3$), 146.9 (s, *ipso*-Ph), 126.2 (d, $^1J_{CH}$ = 155.8, *o*- or *m*-Ph), 127.5 (d, $^1J_{CH}$ = 147.6, *o*- or *m*-Ph), 121.6 (d, $^1J_{CH}$ = 151.3, *p*-Ph), 54.0 (d, partially obscured, Cy−*C*$_1$), 40.0 (s, *C*Me$_3$), 37.1 (t, $^1J_{CH}$ = 117.7, *Cy*), 29.6 (q, $^1J_{CH}$ = 117.3, C*Me*$_3$), 25.9 (t, $^1J_{CH}$ = 118.2, *Cy*), 25.7 (t, $^1J_{CH}$ = 118.2, *Cy*), 21.4 (t, $^1J_{CH}$ = 108.7, *C*H$_2$Ph). Anal. Calcd for $C_{31}H_{45}AlN_2$: C, 78.77; H, 9.60; N, 5.93. Found: C, 78.62; H, 9.58; N, 5.83.

{^{t}BuC(N^{i}Pr)$_2$}Al(CH$_2$CMe$_3$)$_2$ (8a). {^{t}BuC(N^{i}Pr)$_2$}AlCl$_2$ (0.50 g, 1.8 mmol) and LiCH$_2$CMe$_3$ (0.28 g, 3.6 mmol) were mixed as solids in the glovebox. Et$_2$O (40 mL) was added at −78 °C, and the mixture was allowed to warm slowly to room temperature, affording a slurry of a white precipitate in a colorless solution. The mixture was stirred for 18 h, and the volatiles were removed under vacuum. The residue was extracted with pentane, and the extract was taken to dryness under vacuum, affording **7a** as a white solid (0.58 g, 93%). ^{1}H NMR (CD_2Cl_2): δ 4.13 (sept, $^3J_{HH}$ = 6.2, C*H*Me$_2$), 1.39 (s, 9H, C*Me*$_3$), 1.15 (d, $^3J_{HH}$ = 6.3, CH*Me*$_2$), 0.99 (s, 18H, CH$_2$C*Me*$_3$), 0.27 (s, 4H, C*H*$_2$CMe$_3$). ^{13}C NMR (CD_2Cl_2): δ 179.7 (s, *C*CMe$_3$), 46.1 (d, $^1J_{CH}$ = 121.0, *C*HMe$_2$), 40.1 (s, *C*Me$_3$), 35.2 (q, $^1J_{CH}$ = 112.2, CH$_2$C*Me*$_3$), 32.1 (br t, partially obscured, *C*H$_2$CMe$_3$), 31.6 (s, CH$_2$*C*Me$_3$), 29.8 (q, $^1J_{CH}$ = 121.2, C*Me*$_3$), 26.6 (q, $^1J_{CH}$ = 117.9, CH*Me*$_2$). Anal. Calcd for $C_{21}H_{45}AlN_2$: C, 71.54; H, 12.86; N, 7.95. Found: C, 70.46; H, 12.82; N, 7.72.

{^{t}BuC(NCy)$_2$}Al(CH$_2$CMe$_3$)$_2$ (8b). A solution of LiCH$_2$CMe$_3$ (0.43 g, 5.5 mmol) in Et$_2$O (20 mL) was added dropwise at −78 °C to an Et$_2$O solution (30 mL) of {^{t}BuC(NCy)$_2$}AlCl$_2$ (1.0 g, 2.8 mmol). The reaction mixture was allowed to warm slowly to room temperature and was stirred for 15 h. The volatiles were removed under vacuum, the residue was extracted with pentane, and the extract was evaporated to dryness under vacuum to afford {^{t}BuC(NCy)$_2$}Al(CH$_2$CMe$_3$)$_2$ as a white solid (1.13 g, 94%). ^{1}H NMR (CD_2Cl_2): δ 3.63 (m, 2H, *Cy*), 1.86−1.71 (m, 8H, *Cy*), 1.60 (m, 2H, *Cy*), 1.36 (s, 9H, C*Me*$_3$), 1.30−1.09 (m, 8H + 2H, *Cy*), 0.99 (s, CH$_2$C*Me*$_3$), 0.25 (s, 4H, C*H*$_2$CMe$_3$). ^{13}C NMR (CD_2Cl_2): δ 179.7 (s, *C*CMe$_3$), 54.8 (d, $^1J_{CH}$ = 126.8, Cy−*C*$_1$), 40.0 (s, *C*Me$_3$), 37.2 (t, $^1J_{CH}$ = 124.3, *Cy*), 35.2 (q, $^1J_{CH}$ = 117.6, CH$_2$C*Me*$_3$), 32.1 (br t, partially obscured, *C*H$_2$CMe$_3$), 31.6 (s, CH$_2$*C*Me$_3$), 29.8 (q, $^1J_{CH}$ = 119.6, C*Me*$_3$), 26.2 (t, $^1J_{CH}$ = 118.2, *Cy*), 26.1 (t, $^1J_{CH}$ = 118.2, *Cy*). Anal. Calcd for $C_{27}H_{53}AlN_2$: C, 74.95; H, 12.35; N, 6.47. Found: C, 73.87; H, 12.42; N, 6.60.

{MeC(N^{i}Pr)$_2$}$_2$AlCl (9a). This compound was prepared by the procedure described for **4a**, using 0.90 g of AlCl$_3$ (6.8 mmol) and 2.00 g of Li[MeC(N^{i}Pr)$_2$] (13.5 mmol). Removal of the solvent under vacuum afforded crude {MeC(N^{i}Pr)$_2$}$_2$AlCl as an off-white solid. Pure samples were obtained by sublimation (80 °C, 0.005 mmHg) (1.10 g, 47%). ^{1}H NMR (CD_2Cl_2): δ 3.55 (sept, $^3J_{HH}$ = 6.5, 4H, C*H*Me$_2$), 1.94 (s, 6H, C*Me*), 1.16 (d, $^3J_{HH}$ = 6.6, CH*Me*$_2$). ^{13}C NMR (CD_2Cl_2): δ 174.2 (s, *C*Me), 46.1 (d, $^1J_{CH}$ = 127.5, *C*HMe$_2$), 24.4 (q, $^1J_{CH}$ = 120.1, CH*Me*$_2$), 12.0 (q, $^1J_{CH}$ = 122.6, C*Me*). Anal. Calcd for $C_{16}H_{34}AlClN_4$: C, 55.72; H, 9.94; N, 16.24. Found: C, 56.20; H, 9.88; N, 16.12.

{^{t}BuC(N^{i}Pr)$_2$}$_2$AlCl (10a). This compound was prepared by the procedure described for **4a**, using 0.13 g of AlCl$_3$ (13 mmol) and 5.0 g of Li[^{t}BuC(N^{i}Pr)$_2$] (26 mmol). The extract was concentrated and cooled to −30 °C, affording {^{t}BuC(N^{i}Pr)$_2$}$_2$AlCl as pale yellow crystals, which were collected by filtration (2.57 g, 46%). ^{1}H NMR (CD_2Cl_2): δ 4.22 (sept, $^3J_{HH}$ = 6.4, 2H, C*H*Me$_2$), 1.41 (s, 9H, C*Me*$_3$), 1.25 (d, $^3J_{HH}$ = 6.4, 12H, CH*Me*$_2$). ^{13}C NMR (CD_2Cl_2): δ 181.3 (s, *C*CMe$_3$), 45.8 (d, $^1J_{CH}$ = 129.6, *C*HMe$_2$), 39.5 (s, *C*Me$_3$), 30.2 (q, $^1J_{CH}$ = 127.1, C*Me*$_3$), 25.1 (q, $^1J_{CH}$ = 125.5, CH*Me*$_2$). Anal. Calcd for $C_{22}H_{46}AlClN_4$: C, 61.58; H, 10.81; N, 13.06. Found: C, 60.80; H, 10.98; N, 12.76.

{^{t}BuC(NCy)$_2$}$_2$AlCl (10b). This compound was prepared by the procedure described for **4a**, using 0.30 g of AlCl$_3$ (2.3 mmol) in 25 mL of Et$_2$O and 1.2 g of Li[^{t}BuC(NCy)$_2$] (4.6 mmol) in 35 mL of Et$_2$O. The extract was concentrated and cooled to 0 °C, yielding pure {^{t}BuC(N(Cy)$_2$}$_2$AlCl as yellow crystals, which were collected by filtration (0.25 g, 19%). ^{1}H NMR (CD_2Cl_2): δ 3.69 (br m, 2H, *Cy*), 1.38 (s, 9H, C*Me*$_3$), 1.86−1.80 (m, 4H, *Cy*), 1.70 (m, 8H, *Cy*), 1.57−1.55 (m, 2H, *Cy*), 1.15 (m, 4H + 2H, *Cy*). ^{13}C NMR (CD_2Cl_2): δ 181.3 (s, *C*CMe$_3$), 54.9 (d, $^1J_{CH}$ = 138.7, Cy−*C*$_1$), 39.5 (s, *C*Me$_3$), 34.9 (t, $^1J_{CH}$ = 127.9, *Cy*), 30.3 (q, $^1J_{CH}$ = 127.7, C*Me*$_3$), 26.5 (t, $^1J_{CH}$=125.7, *Cy*), 26.0 (t, $^1J_{CH}$=125.7, *Cy*). Anal. Calcd for $C_{34}H_{62}AlClN_4$: C, 69.29; H, 10.60; N, 9.51. Found: C, 69.46; H, 10.58; N, 9.34.

X-ray Structural Determinations. The structures of **1b**, **3d**, **5a**,**b**, **6b**, **8b**, and **10a**,**b** were determined at the University of Iowa by D. C. Swenson. The structures of **4a** and **9a** were determined at the University of Minnesota by V. G. Young. Crystal data, data collection details, and solution and refinement procedures are collected in Tables 1, 4, and 6. Additional comments specific to each structure follow.

{MeC(NCy)$_2$}AlMe$_2$ (1b): crystals were obtained by slow sublimation (55 °C, 0.005 mmHg, 3 days). All H-atom isotropic thermal parameters were refined independently except U_{iso} (H8A) = U_{iso} (H8B), U_{iso} (H9A) = U_{iso} (H9B), U_{iso} (H10A) = U_{iso} (H10B), U_{iso} (H11A) = U_{iso} (H11B), and U_{iso} (H12A) = U_{iso} (H12B). No other restraints or constraints were imposed.

[Li(^{t}BuCN){μ-N(SiMe$_3$)$_2$}]$_2$ (3d): crystals were grown by crystallization from pentane at −30 °C. Unreasonably large thermal parameters for the ^{t}Bu-methyl C atoms were observed suggesting disorder. These large thermal parameters were reduced with refinement of the C_5H_9 portion as rigid groups with disorder. Two sites for the N-atoms were allowed, with the Li−N, Li−N′ and N−C, N′−C′ distances restrained to be the same. As the sites refined to values of close proximity, the same anisotropic thermal parameters were used for each site. Rigid bond restraints were applied to the thermal parameters of the ^{t}Bu groups. The corresponding C atoms of disorder groups that refined to distances C−C′ < 0.5 Å were assigned the same thermal parameters. A similarity restraint was applied to the thermal parameters of the C atoms where 0.5 Å < C−C′ < 1.2 Å. H atoms were included at calculated positions, and the same thermal parameter was used for each H atom of a methyl group and its disorder mate. Each group was allowed to "expand" or "contract" slightly to compensate for high thermal motion. The coordinates and isotropic thermal parameters of all methyl H atoms of the four SiMe$_3$ groups refined to reasonable values. The relative occupancy for the two orientations of the Li(1) nitrile group (NC(1), C(2)−C(6) and NC(1′), C(2′)−C(6′)) refined to 0.715(6) and 0.285(6), where a rotation of approximately 30° about the NC(1)−C(2) bond transforms the major orientation to the minor one. For the Li(2) nitrile group (NC(2), C(12)−C(16) and NC(2′), C(12′)−C(16′)), occupancies refined to 0.459(6) and 0.541(6), where again a rotation of approximately 30° about the NC(2)−C(12) bond transforms the one orientation to the other.

{MeC(N^{i}Pr)$_2$}AlCl$_2$ (4a): crystals were obtained by sublimation (50 °C, 0.005 mmHg). All non-H atoms were refined anisotropically, and all H atoms were placed in ideal positions and refined as riding atoms with group isotropic displacement factors.

{^{t}BuC(N^{i}Pr)$_2$}AlCl$_2$ (5a): crystals were grown from a saturated pentane solution cooled to 0 °C. The structure is disordered in three ways. The ^{t}Bu group is present in two

orientations with relative occupancies of 0.85(1) and 0.15(1). The rotation angle about the C(5)−C(6) bond that positions one disorder orientation to the other is necessarily 180°. The H atoms for each disordered ^{t}Bu group were included and given the same isotropic thermal parameter, and the C−H distances were restrained to be the same. The second disorder is in the C(1), H(1), C(2), C(2′) ^{i}Pr group, with disorder necessarily 50:50 by symmetry. The crystallographic mirror plane ($x = 0.25$) generates the other disorder orientation, and a rotation of approximately 30° about N(1)−C(1) and 25° about Al−N(1) positions the C(1), H(1), C(2), C(2′) orientation to C(1A), H(1A), C(2A), C(2′A). The C(1), H(1), C(2), C(2′) atoms were refined as a rigid group, and the H atoms were included at tetrahedral positions. The C−H distances for C(1)−H(1) and the methyl groups were allowed to refine, but were restrained to be the same for all methyl H atoms. The same isotropic thermal parameter was given to all methyl H atoms, and U_{iso} was allowed to refine for H(1). The third disorder is in the C(4) methyl hydrogens, with two locations detected with the relative occupancy refined to 0.42(6) and 0.58(6). The C−H distances were restrained to be the same, and the same U_{iso} was given to all H atoms.

{^{t}BuC(NCy)$_2$}AlCl$_2$ (5b): crystals were grown from a saturated toluene solution cooled to 0 °C. The structure was found to be disordered. A crystallographic two-fold axis passes through Al, C(21), and C(22), imposing two-fold symmetry and necessitating disorder of the ^{t}Bu group. There is additional disorder involving the C(1)−C(6) cyclohexyl group and the C(23) methyl group, with the relative occupancies being refined to 0.65(2) and 0.35(2). The minor conformer can be approximated by rotating the cyclohexyl group 36° counterclockwise about the N(1)−C(1) bond and twisting the N(1)−C(21)−C(22)−C(23) torsion angle 27° clockwise. The correlation between the cyclohexyl and methyl group orientations can be understood by examination of relevant nonbonding intramolecular close contacts and bond angles. The C(23) methyl group and C(1) of the cyclohexyl group are close to the plane defined by Al, N(1), C(21), C(22), N(1a), where N(1a) is generated by symmetry. The close contact between C(23) and N(1), C(1) forces the C(21)−C(22)−C(23) angle to be greater than tetrahedral. The H(23B) and H(23C) atoms straddle the N(1)−C(1) bond, and H(1) is approximately equidistant from these two methyl H atoms. The C(23′) methyl hydrogens are rotated to preserve the "interlocking" arrangement. The cyclohexyl group adopts the chair conformation in both disorder structures. A rigid bond restraint was applied to the anisotropic thermal parameters of each disorder group. The bonding and nonbonding contacts of the corresponding atoms in the two disorder groups were restrained to be the same. The C−H distances and H atom isotropic thermal parameters for each methylene unit of the cyclohexyl group were allowed to vary during refinement, with the corresponding values of the disorder groups restrained to be the same. The C(1′)−H(1′) distance was restrained to be the same as the C(1)−H(1) distance, and U_{iso} for H(1′) was set equal to that of H(1) and refined. A C−H distance and U_{iso} was refined for each methyl group, and rotation about each C−C (methyl) bond was allowed. The U_{iso} value for the C(23′) H atoms was set equal to that of the C(23) H atoms.

{^{t}BuC(NCy)$_2$}AlMe$_2$ (6b): crystals were grown by cooling a warm (40 °C) saturated pentane solution to room temperature. The coordinates and isotropic thermal parameters of all H atoms refined to reasonable values.

{^{t}BuC(NCy)$_2$}Al(CH$_2$CMe$_3$)$_2$ (8b): crystals were grown from a concentrated pentane solution at −30 °C. The structure shows disorder in each of the neopentyl ligands. The C(18)−C(22) neopentyl ligand was modeled with two orientations, and the C(23)−C(27) neopentyl group was modeled with three orientations, with each neopentyl ligand being refined as a rigid group. For C(18)−C(22), the relative occupancy of the major orientation to the minor one, C(18′)−C(22′), is 0.737:0.263. A clockwise rotation of 35° about Al−C(18) converts the major orientation into the minor one. H atoms were included at calculated positions with the riding atom model, and C atoms were allowed to have anisotropic thermal parameters restrained with a rigid bond restraint. The thermal parameters of C(18′), C(19′), and C(22′) were set equal to those of C(18), C(19), and C(22), respectively, due to their close proximity. The three orientations of the second neopentyl ligand, C(23)−C(27), C(23′)−C(27′), and C(23″)−C(27″), have relative occupancies of 0.490, 0.340, and 0.171, respectively. A rotation of ca. 40° about C(23)−C(24) positions the first orientation to the second; another 40° rotation gives the third orientation. Inclusion of the H atoms and refinement of the C atom anisotropic thermal parameters were treated in a manner similar to that discussed for the C(18)−C(22) neopentyl ligand. C(23), C(23′), and C(23″) were assigned the same thermal parameters, as were C(24), C(24′), and C(24″) due to their close proximity. The H atom positions and isotropic thermal parameters of the two cyclohexyl groups, C(1)−C(6) and C(7)−C(12), and of the ^{t}Bu group, C(14)−C(17), were refined.

{MeC(N^{i}Pr)$_2$}$_2$AlCl (9a): crystals were grown by slow sublimation (80 °C, 0.005 mmHg, 5 days). Non-H atoms were refined anisotropically. All H atoms were placed in ideal positions and refined as riding atoms with group isotropic displacement factors.

{^{t}BuC(N^{i}Pr)$_2$}$_2$AlCl (10a): crystals were grown from a saturated pentane solution at −30 °C. The C−H bond directions were constrained to give tetrahedral angles. The C(3) C−H bond distances were allowed to refine independently, and a C−H distance was determined for each CH_3 group. Each methyl group was allowed to refine by rotation about the $-CH_3$ bond. All H atom isotropic thermal parameters were refined independently.

{^{t}BuC(NCy)$_2$}$_2$AlCl (10b): crystals were grown from a saturated pentane solution at −30 °C. The structure was found to contain a molecule of pentane situated near an inversion center that is necessarily disordered. The C atoms of the solvent molecule were refined with anisotropic thermal parameters subject to the rigid bond restraint. The C−C distances were restrained to 1.54 Å, and the C(1)−C(2)−C(3) distances were restrained to be the same. H atoms were included in the solvent molecule at calculated positions with the riding atom model.

Acknowledgment. This work was supported by DOE Grant DE-FG02−88ER13935. MPC was supported in part by a NATO postdoctoral research fellowship.

Supporting Information Available: Tables of atomic coordinates, isotropic displacement parameters, anisotropic displacement parameters, bond distances and bond angles, and hydrogen atom coordinates and listings of MS and IR data for **1b**, **3d**, **4a**, **5a**, **5b**, **6b**, **8b**, **9a**, **10a**, and **10b** (81 pages). Ordering information is given on any current masthead page.

OM9706323